Copyright © 1978, by the author(s).
All rights reserved.

Permission to make digital or hard copies of all or part of this work for personal or classroom use is granted without fee provided that copies are not made or distributed for profit or commercial advantage and that copies bear this notice and the full citation on the first page. To copy otherwise, to republish, to post on servers or to redistribute to lists, requires prior specific permission.

TWO NEW ALGORITHMS FOR OBTAINING PERIODIC SOLUTIONS OF NONLINEAR SYSTEMS

by

L. O. Chua and A. Ushida

Memorandum No. UCB/ERL M78/31

23 March 1978

ELECTRONICS RESEARCH LABORATORY

College of Engineering
University of California, Berkeley
94720

TWO NEW ALGORITHMS FOR OBTAINING PERIODIC SOLUTIONS OF NONLINEAR SYSTEMS[†]

Leon O. Chua and Akio Ushida[††]

ABSTRACT

Two new algorithms based on the "shooting method" for obtaining periodic solutions of nonlinear systems described by implicit differential-algebraic equations are presented. The first algorithm is based on an n-dimensional secant method and requires only one transient analysis per iteration (compared to n+1 analyses needed in the discretized Newton method) after the initial step. The second algorithm is globally convergent under rather mild conditions and is based on the switching parameter approach. This algorithm is particularly useful for solving systems having multiple periodic solutions. Examples taken from the area of nonlinear oscillation show that multivalued frequency response characteristics containing jump phenomena of nonlinear systems can be accurately derived using this algorithm.

[†]Research supported in part by the Office of Naval Research Contract N00014-76-0572 and the National Science Foundation Grant ENG77-22745.

[††]Leon O. Chua is with the Department of Electrical Engineering and Computer Sciences and the Electronics Research Laboratory, University of California, Berkeley, California 94720.

A. Ushida is with the Department of Electrical Engineering, Technical College of Tokushima University, Tokushima, Japan.

I. INTRODUCTION

Much research has been done on the development of efficient computer algorithms for finding the periodic steady state solutions of both autonomous and non-autonomous nonlinear systems. The algorithms that have been developed can be classified into two basic categories. The first [1-5] is based on the shooting method, while the second [6-9] is based on the harmonic balance method. The first approach is general but could be quite time consuming for large systems because each iteration requires numerically integrating the system's differential equations (over one period) a total of (n+1) times, where n is the number of state variables. The second approach is practical only if the number of harmonic components in the periodic solution is small. If the number of nonlinear elements is also small compared to the number of linear elements, the recent method reported in [8-9] is generally more efficient. One serious drawback of the harmonic balance approach is that there is no systematic procedure for identifying which harmonic components are significant, let alone their approximate amplitudes.

Our objective in this paper is to present two new algorithms for implementing the shooting method. Since state equations for nonlinear networks are generally difficult, if not impossible, to formulate in explicit analytical form [10], our algorithm will be developed for the following more general system of implicit differential-algebraic equations

$$\underset{\sim}{f}(\dot{\underset{\sim}{x}},\underset{\sim}{x},\underset{\sim}{y},t) = \underset{\sim}{0} \qquad (1)$$

where $\underset{\sim}{x} \in \mathbb{R}^n$, $\underset{\sim}{y} \in \mathbb{R}^m$, and $\underset{\sim}{f}$: $\mathbb{R}^{2n+m+1} \rightarrow \mathbb{R}^n$.
The equations of any lumped nonlinear network can be easily cast in this form using the Tableau formulation [10]. Such equations are generally sparse and hence sparse matrix techniques should be used in any general purpose simulation program. For relatively small circuits, however, where the improvement using sparse matrix techniques is not decisive, it would be advantageous to reduce (1) further by minimizing the number of "non-state variables." An explicit form of this "reduced" system of implicit equations is derived in Appendix 1 for an important class of nonlinear networks. Most networks of practical interest can be described in this reduced implicit form. In particular, all examples in this paper are formulated in this form.

Both autonomous (unforced) and non-autonomous (forced) systems will be considered. In the former, the variable "t" is absent in (1) and in the latter,

$\underset{\sim}{f}(\cdot)$ is "T-periodic" in the sense that

$$\underset{\sim}{f}(\dot{\underset{\sim}{x}},\underset{\sim}{x},\underset{\sim}{y},t) = \underset{\sim}{f}(\dot{\underset{\sim}{x}},\underset{\sim}{x},\underset{\sim}{y},t+T) \tag{2}$$

for all t. The shooting method for solving (1) via the discretized Newton iteration[1] is virtually identical to that given in [1-3], and involves solving the implicit system (1) over one period a total of n+1 times per iteration. This is implemented in [3] by solving "n" sensitivity networks, in addition to the original network, over one period per iteration. In Section II, we will develop an explicit formula for implementing the discretized Newton method directly, that is, without using sensitivity networks. This formula allows us to implement the shooting method using (1) directly and therefore is applicable to any such implicit systems regardless of whether they pertain to a circuit or not. Instead of solving (n+1) networks over [0,T], this formula requires that we solve (1) over [0,T] (n+1) times per iteration. Even if (1) pertains to a circuit, this formula will still be useful in the event that the circuit contains elements, such as nonlinear controlled sources [11], where a sensitivity circuit model is not available. This explicit formula can also be used for developing a general purpose computer subroutine for solving any implicit system of differential-algebraic equations.

The main results of this paper are given in Sections III and IV. An explicit formula for solving (1) via the secant method is developed in Section III. This method consists of solving (1) over [0,T] only once per iteration, after an initialization step where (1) is solved over [0,(n+1)T]. Although any efficient method for solving (1) can be used, our experience shows that the backward-differentiation formula (BDF) [10] to be particularly well-suited for this purpose. Since most of the time used in implementing the shooting method is spent in solving (1), it is not surprising that the secant method turns out to be more efficient than the discretized Newton iteration of Section II. This fact will be established in Section III.

Both the Newton and the secant iterations will generally converge only if the initial guess $\underset{\sim}{x}^0(0)$ is close to a solution point. No general algorithm currently exists for choosing a suitable initial guess. To overcome this

---

[1] By discretized Newton iteration, we mean the Newton-Raphson method where the Jacobian matrix is evaluated by numerical differentiation.

problem, a globally convergent algorithm based on the switching parameter approach [12] will be proposed in Section IV. Under rather mild assumptions, this algorithm always converges regardless of the choice of the initial guess. Moreover, if the system has more than one periodic solution, as is common in many nonlinear systems [6], this algorithm will find multiple solution points, each one giving rise to a distinct periodic solution. Since it is applicable regardless of whether the solution is stable or unstable, this algorithm provides the only systematic approach for deriving the "multivalued" frequency and amplitude response curves associated with ferroresonance and other jump phenomena observed in many nonlinear circuits and systems.

Several examples illustrating the applications of the algorithms in Sections III and IV are presented in Section V. The advantages of these algorithms are clearly demonstrated by these examples.

II. EXPLICIT FORM OF DISCRETIZED NEWTON ITERATION

Let $\left(\underset{\sim}{x}^0(t),\underset{\sim}{y}^0(t)\right)$ be a solution of (1) with initial value $\underset{\sim}{x}^0(0)$. Let

$$\underset{\sim}{x}(0) = \underset{\sim}{x}^0(0) + \underset{\sim}{\eta}(0), \quad \|\underset{\sim}{\eta}(0)\| \ll 1 \tag{3}$$

be a "perturbed" initial value and let

$$\underset{\sim}{x}(t) = \underset{\sim}{x}^0(t) + \underset{\sim}{\eta}(t), \quad \underset{\sim}{y}(t) = \underset{\sim}{y}^0(t) + \underset{\sim}{\gamma}(t) \tag{4}$$

denote the corresponding solution. Applying Taylor expansion in (1) about the point $\left(\underset{\sim}{x}^0(t),\underset{\sim}{y}^0(t),t\right)$, we obtain

$$\underset{\sim}{f}\left(\dot{\underset{\sim}{x}}^0(t),\underset{\sim}{x}^0(t),\underset{\sim}{y}^0(t),t\right) + \left[\frac{\partial \underset{\sim}{f}}{\partial \dot{\underset{\sim}{x}}} \frac{\partial \underset{\sim}{f}}{\partial \underset{\sim}{x}} \frac{\partial \underset{\sim}{f}}{\partial \underset{\sim}{y}}\right]\begin{bmatrix}\dot{\underset{\sim}{\eta}}(t)\\ \underset{\sim}{\eta}(t)\\ \underset{\sim}{\gamma}(t)\end{bmatrix} + 0\left(\|\dot{\underset{\sim}{\eta}}(t)\|^2,\|\underset{\sim}{\eta}(t)\|^2,\|\underset{\sim}{\gamma}(t)\|^2\right) = \underset{\sim}{0} \tag{5}$$

where the partial derivatives are evaluated at $\left(\underset{\sim}{x}^0(t),\underset{\sim}{y}^0(t)\right)$. The first term in (5) is zero by definition of $\underset{\sim}{x}^0(t)$ and $\underset{\sim}{y}^0(t)$. If we neglect the higher order terms, (5) can be recast as follows:

$$\begin{bmatrix}\dot{\underset{\sim}{\eta}}(t)\\ \underset{\sim}{\gamma}(t)\end{bmatrix} = -\left[\frac{\partial \underset{\sim}{f}}{\partial \dot{\underset{\sim}{x}}} \frac{\partial \underset{\sim}{f}}{\partial \underset{\sim}{y}}\right]^{-1}\left[\frac{\partial \underset{\sim}{f}}{\partial \underset{\sim}{x}}\right]\underset{\sim}{\eta} \triangleq \begin{bmatrix}\underset{\sim}{A}(t)\\ \underset{\sim}{B}(t)\end{bmatrix}\underset{\sim}{\eta} \tag{6}$$

The solution to the linear time-varying system

$$\dot{\underset{\sim}{\eta}}(t) = \underset{\sim}{A}(t)\underset{\sim}{\eta}(t) \tag{7}$$

is given by

$$\underset{\sim}{\eta}(t) = \underset{\sim}{X}^0(t)\underset{\sim}{\eta}(0) \tag{8}$$

where $\underset{\sim}{X}^0(t)$ is a fundamental matrix solution of (7) [13]. It follows from (4) and (8) that

$$\underset{\sim}{x}(T) = \underset{\sim}{X}^0(T)\underset{\sim}{\eta}(0) + \underset{\sim}{x}^0(T) \tag{9}$$

Now if we assume $\underset{\sim}{x}(0)$ is an initial value which gives rise to a T-periodic solution, i.e., $\underset{\sim}{x}(0) = \underset{\sim}{x}(T)$, then we can substitute (3) for $\underset{\sim}{x}(T)$ in (9) and obtain

$$\underset{\sim}{\eta}(0) = -[\underset{\sim}{1}-\underset{\sim}{X}^0(T)]^{-1}[\underset{\sim}{x}^0(0)-\underset{\sim}{x}^0(T)] \tag{10}$$

Substituting (10) into (3), we obtain

$$\underset{\sim}{x}(0) = \underset{\sim}{x}^0(0) - [\underset{\sim}{1}-\underset{\sim}{X}^0(T)]^{-1}[\underset{\sim}{x}^0(0)-\underset{\sim}{x}^0(T)] \tag{11}$$

Hence (11) gives us a formula for computing an initial condition which gives rise to a T-periodic solution $\underset{\sim}{x}(t)$ provided the higher order terms in (4) are zero, i.e., provided $\underset{\sim}{f}(\cdot)$ is linear in $\dot{\underset{\sim}{x}}$, $\underset{\sim}{x}$ and $\underset{\sim}{y}$. If $\underset{\sim}{f}(\cdot)$ is nonlinear, (11) is no longer exact but it should give a good approximation to the correct initial value $\hat{\underset{\sim}{x}}(0)$ if the perturbation $\underset{\sim}{\eta}(0)$ is small. This suggests the following basic iteration formula

$$\boxed{\underset{\sim}{x}^{j+1}(0) = \underset{\sim}{x}^j(0) - [\underset{\sim}{1}-\underset{\sim}{X}^j(T)]^{-1}[\underset{\sim}{x}^j(0)-\underset{\sim}{x}^j(T)],\ j \geq 0} \tag{12}$$

Now if we define

$$\underset{\sim}{F}\left(\underset{\sim}{x}(0)\right) \triangleq \underset{\sim}{x}(0) - \underset{\sim}{x}\left(T;\underset{\sim}{x}(0)\right) \tag{13}$$

then (12) is precisely the Newton-Raphson formula for solving $\underset{\sim}{F}(\underset{\sim}{x}(0)) = \underset{\sim}{0}$ because it can be easily shown that [1]

$$\underset{\sim}{X}^j(T) = \frac{\partial \underset{\sim}{x}^j\left(T;\underset{\sim}{x}(0)\right)}{\partial \underset{\sim}{x}(0)} \tag{14}$$

It is well known that if the initial guess $\underset{\sim}{x}(0)$ is sufficiently close to an exact initial value $\hat{\underset{\sim}{x}}(0)$ which gives rise to a T-periodic solution in (1), then (12) converges quadratically to $\hat{\underset{\sim}{x}}(0)$ as $j \to \infty$ [1,14]. Hence, two problems must be solved before (12) can be implemented efficiently: 1) choose a suitable initial guess and 2) find an efficient method to compute for the fundamental matrix solution in (14). The first problem will be considered in Section IV. The second problem is solved in [3] by finding the transient response over [0,T] of (n+1) networks -- the original network and its associated n sensitivity networks. Rather than computing $\underset{\sim}{X}^j(T)$, we will now derive a formula which gives $[\underset{\sim}{1}-\underset{\sim}{X}^j(T)]$ explicitly by solving (1) over [0,T] (n+1) times.

Let $\underset{\sim}{x}(0)$ be an initial guess and let

$$\underset{\sim}{he}_i \triangleq h[0\ 0\ldots0\ \underset{\uparrow i\text{th component}}{1}\ 0\ldots0]^T, \quad i = 1,2,\ldots,n \tag{15}$$

denote a set of "n" perturbation vectors where $h << 1$.[2] Hence (3) assumes the form[3]

$$\overset{i}{\underset{\sim}{x}}(0) = \underset{\sim}{x}(0) + \underset{\sim}{he}_i \tag{16}$$

Now if h is sufficiently small, the solution (4) at t = T corresponding to these initial conditions can be approximated by

$$\overset{i}{\underset{\sim}{x}}(T) = \underset{\sim}{x}(T) + h\underset{\sim}{X}(T)\underset{\sim}{e}_i, \quad i = 1,2,\ldots,n \tag{17}$$

Subtracting (17) from (16), we obtain

$$[\underset{\sim}{1}-\underset{\sim}{X}(T)]\underset{\sim}{he}_i = [\overset{i}{\underset{\sim}{x}}(0)-\overset{i}{\underset{\sim}{x}}(T)] - [\underset{\sim}{x}(0)-\underset{\sim}{x}(T)] = -[\overset{i}{\underset{\sim}{x}}(T)-\underset{\sim}{x}(T)] + [\overset{i}{\underset{\sim}{x}}(0)-\underset{\sim}{x}(0)]$$

$$= -[\overset{i}{\underset{\sim}{x}}(T)-\underset{\sim}{x}(T)] + \underset{\sim}{he}_i, \quad i = 1,2,\ldots,n \tag{18}$$

Now if we form an nxn matrix whose ith column is given by $[\underset{\sim}{1}-\underset{\sim}{X}(T)]\underset{\sim}{he}_i$, then it follows from (15) that

$$[\underset{\sim}{1}-\underset{\sim}{X}(T)] = \frac{1}{h}\begin{bmatrix} h-[\overset{1}{x}_1(T)-x_1(T)] & -[\overset{2}{x}_1(T)-x_1(T)] & \cdots & -[\overset{n}{x}_1(T)-x_1(T)] \\ -[\overset{1}{x}_2(T)-x_2(T)] & h-[\overset{2}{x}_2(T)-x_2(T)] & \cdots & -[\overset{n}{x}_2(T)-x_2(T)] \\ \vdots & \vdots & \vdots & \vdots \\ -[\overset{1}{x}_n(T)-x_n(T)] & -[\overset{2}{x}_n(T)-x_n(T)] & \cdots & h-[\overset{n}{x}_n(T)-x_n(T)] \end{bmatrix} \tag{19}$$

Since $\underset{\sim}{x}(T)$ is obtained by solving (1) over [0,T] with initial value $\underset{\sim}{x}(0)$, and since $\overset{i}{\underset{\sim}{x}}(T)$ is obtained by solving (1) over [0,T] with initial value $\overset{i}{\underset{\sim}{x}}(0)$, $i = 1,2,\ldots,n$, it is clear that $[\underset{\sim}{1}-\underset{\sim}{X}(T)]$ is determined by solving (1) n+1 times over [0,T].[4] Substituting (19) in (12), we obtain the following explicit discretized Newton iteration formula:

---

[2] All examples in Section V assume h = 0.01.

[3] We have chosen the slightly clumsy notation $\overset{i}{\underset{\sim}{x}}(0)$ to denote the initial condition corresponding to $\underset{\sim}{he}_i$ because $\overset{j}{x}_k(0)$ will be used later to denote the kth component of $\underset{\sim}{x}(0)$ at the jth iteration.

[4] The backward-differentiation formula (BDF) [10] is ideally suited for solving the implicit system of differential algebraic equations in (1).

$$\begin{bmatrix} x_1^{j+1}(0) \\ x_2^{j+1}(0) \\ \vdots \\ x_n^{j+1}(0) \end{bmatrix} = \begin{bmatrix} x_1^{j}(0) \\ x_2^{j}(0) \\ \vdots \\ x_n^{j}(0) \end{bmatrix} - \frac{1}{h} \begin{bmatrix} h-[{}^1x_1^j(T)-x_1^j(T)] & -[{}^2x_1^j(T)-x_1^j(T)] & \cdots & -[{}^nx_1^j(T)-x_1^j(T)] \\ -[{}^1x_2^j(T)-x_2^j(T)] & h-[{}^2x_2^j(T)-x_2^j(T)] & \cdots & -[{}^nx_2^j(T)-x_2^j(T)] \\ \vdots & \vdots & \vdots & \vdots \\ -[{}^1x_n^j(T)-x_n^j(T)] & -[{}^2x_n^j(T)-x_n^j(T)] & \cdots & h-[{}^nx_n^j(T)-x_n^j(T)] \end{bmatrix}^{-1} \begin{bmatrix} x_1^j(0)-x_1^j(T) \\ x_2^j(0)-x_2^j(T) \\ \vdots \\ x_n^j(0)-x_n^j(T) \end{bmatrix}, \quad j = 0,1,2,\ldots \tag{20}$$

The discretized Newton iteration algorithm can now be summarized as follows:

Step 0. Set $j = 0$.

Step 1. For given initial state $\underset{\sim}{x}^j(0)$, compute $\underset{\sim}{x}^j(T)$.

Step 2. Go to step 5 if $\|\underset{\sim}{x}^j(0)-\underset{\sim}{x}^j(T)\| < \varepsilon$, where ε is a sufficiently small positive number to estimate the error of solution.

Step 3. Choose n initial states ${}^i\underset{\sim}{x}^j(0) = \underset{\sim}{x}^j(0) + h\underset{\sim}{e}_i$, $i = 1,2,\ldots,n$, and compute corresponding ${}^i\underset{\sim}{x}^j(T)$, where h is a small constant.

Step 4. Compute $\underset{\sim}{x}^{j+1}(0)$ from (20). Go to step 1.

Step 5. Stop.

The above algorithm is valid so long as the matrix $[\underset{\sim}{1}-\underset{\sim}{X}^j(T)]$ in (20) is non-singular, and provided that (1) has at least one T-periodic solution. It is clear that the algorithm in [3] is a circuit implementation of (20).

III. EXPLICIT FORM OF SECANT METHOD

A. Non-Autonomous System

The one-dimensional secant method for solving $F(x(0)) = 0$ ($F(\cdot)$ is defined in (13)) is given by [14-15]:

$$x^{j+1}(0) = x^j(0) - \left[\frac{F\left(x^{j-1}(0)\right)-F\left(x^j(0)\right)}{x^{j-1}(0)-x^j(0)}\right]^{-1} F\left(x^j(0)\right) \tag{21}$$

where $j = 1,2,\ldots$. The geometrical interpretation of (21) is shown in Fig. 1 where the expression enclosed within the bracket in (21) is the slope of the secant line passing through the two points $(x^0(0),F(x^0(0)))$ and $(x^1(0),F(x^1(0)))$. Notice that in the limit where $x^1(0)$ tends toward $x^0(0)$, (21) reduces to the Newton-Raphson method. Observe that except for the initial step where two function evaluations are needed, $(F(x^0(0))$ and $F(x^1(0)))$, each succeeding iteration requires only one function evaluation, as compared to two in the discretized Newton method.

To derive the n-dimensional version of the secant method, let us assume "n" consecutive initial states $\underset{\sim}{x}^0(0)$, $\underset{\sim}{x}^1(0) \triangleq \underset{\sim}{x}(T)$, $\underset{\sim}{x}^2(0) \triangleq \underset{\sim}{x}^1(T) = \underset{\sim}{x}(2T)$, ..., $\underset{\sim}{x}^m(0) \triangleq \underset{\sim}{x}^{m-1}(T) = \underset{\sim}{x}(mT)$, $m = 1,2,\ldots,n+1$, where $\underset{\sim}{x}(t)$ is the solution of (1)

corresponding to the initial condition $\underset{\sim}{x}(0) = \underset{\sim}{x}^0(0)$. Now for each initial state $\underset{\sim}{x}^j(0)$, $j \geq n$, choose two successive states $\underset{\sim}{x}^k(0)$ and $\underset{\sim}{x}^{k+1}(0)$, where $j - n \leq k \leq j - 1$. Let $\underset{\sim}{\eta}^k(0)$ denote the difference between $\underset{\sim}{x}^k(0)$ and $\underset{\sim}{x}^j(0)$, and let $\underset{\sim}{\eta}^{k+1}(0)$ denote the difference between $\underset{\sim}{x}^{k+1}(0)$ and $\underset{\sim}{x}^j(0)$; i.e.,

$$\underset{\sim}{x}^k(0) = \underset{\sim}{x}^j(0) + \underset{\sim}{\eta}^k(0) \tag{22}$$

$$\underset{\sim}{x}^{k+1}(0) = \underset{\sim}{x}^j(0) + \underset{\sim}{\eta}^{k+1}(0) \tag{23}$$

If we neglect the higher order terms in (5) as in Section II, the solutions $\underset{\sim}{x}^k(t)$ and $\underset{\sim}{x}^{k+1}(t)$ at $t = T$ corresponding to the initial values $\underset{\sim}{x}^k(0)$ and $\underset{\sim}{x}^{k+1}(0)$ are given respectively by:

$$\underset{\sim}{x}^k(T) = \underset{\sim}{x}^j(T) + \underset{\sim}{X}^j(T)\underset{\sim}{\eta}^k(0) \tag{24}$$

$$\underset{\sim}{x}^{k+1}(T) = \underset{\sim}{x}^j(T) + \underset{\sim}{X}^j(T)\underset{\sim}{\eta}^{k+1}(0) \tag{25}$$

Here, $\underset{\sim}{X}^j(t)$ is the fundamental matrix solution of (7) where $\underset{\sim}{A}(t)$ is evaluated at $\underset{\sim}{x} = \underset{\sim}{x}^j(t)$. If we substract the difference between (22) and (24) from that between (23) and (25), we would obtain

$$\begin{aligned}
&\left[\underset{\sim}{x}^k(0)-\underset{\sim}{x}^k(T)\right] - \left[\underset{\sim}{x}^{k+1}(0)-\underset{\sim}{x}^{k+1}(T)\right] \\
&= \left[\underset{\sim}{x}^j(0)+\underset{\sim}{\eta}^k(0)-\underset{\sim}{x}^j(T)-\underset{\sim}{X}^j(T)\underset{\sim}{\eta}^k(0)\right] - \left[\underset{\sim}{x}^j(0)+\underset{\sim}{\eta}^{k+1}(0)-\underset{\sim}{x}^j(T)-\underset{\sim}{X}^j(T)\underset{\sim}{\eta}^{k+1}(0)\right] \\
&= \left[1-\underset{\sim}{X}^j(T)\right]\left[\underset{\sim}{\eta}^k(0)-\underset{\sim}{\eta}^{k+1}(0)\right] = \left[1-\underset{\sim}{X}^j(T)\right]\left[\underset{\sim}{x}^k(0)-\underset{\sim}{x}^{k+1}(0)\right]
\end{aligned} \tag{26}$$

Since $\underset{\sim}{x}^m(0) = \underset{\sim}{x}^{m-1}(T)$, it follows from (13) that

$$\underset{\sim}{F}\left(\underset{\sim}{x}^k(0)\right) - \underset{\sim}{F}\left(\underset{\sim}{x}^{k+1}(0)\right) = \left[\underset{\sim}{x}^k(0)-\underset{\sim}{x}^k(T)\right] - \left[\underset{\sim}{x}^{k+1}(0)-\underset{\sim}{x}^{k+1}(T)\right] \tag{27}$$

Now if we form an nxn matrix whose columns are given by (26), where k ranges from j-n to j-1, would obtain

$$\underset{\sim}{\Gamma}^j = [\underset{\sim}{1}-\underset{\sim}{X}^j(T)]\underset{\sim}{H}^j \tag{28}$$

where

$$\underset{\sim}{H}^j \triangleq \left[\left(\underset{\sim}{x}^{j-n}(0)-\underset{\sim}{x}^{j-n+1}(0)\right) \quad \left(\underset{\sim}{x}^{j-n+1}(0)-\underset{\sim}{x}^{j-n+2}(0)\right) \quad \cdots \left(\underset{\sim}{x}^{j-1}(0)-\underset{\sim}{x}^{j}(0)\right)\right] \tag{29}$$

$$\underset{\sim}{\Gamma}^j \triangleq \left[\left[\underset{\sim}{F}\left(\underset{\sim}{x}^{j-n}(0)\right) - \underset{\sim}{F}\left(\underset{\sim}{x}^{j-n+1}(0)\right)\right]\left[\underset{\sim}{F}\left(\underset{\sim}{x}^{j-n+1}(0)\right) - \underset{\sim}{F}\left(\underset{\sim}{x}^{j-n+2}(0)\right)\right] \cdots \left[\underset{\sim}{F}\left(\underset{\sim}{x}^{j-1}(0)\right) - \underset{\sim}{F}\left(\underset{\sim}{x}^{j}(0)\right)\right]\right] \tag{30}$$

It follows from (28) that if the matrix $\underset{\sim}{\Gamma}^j$ is nonsingular, then

$$[\underset{\sim}{1}-\underset{\sim}{X}^j(T)]^{-1} = \underset{\sim}{H}^j(\underset{\sim}{\Gamma}^j)^{-1} \tag{31}$$

Again if the function $\underset{\sim}{f}(\cdot)$ in (1) is linear, then we can substitute (31) into (11) and compute the initial value $\underset{\sim}{x}(0)$ which gives rise to a T-periodic solution exactly. If $\underset{\sim}{f}(\cdot)$ is not linear, we can substitute (31) into (12) to obtain the following iteration algorithm:

$$\underset{\sim}{x}^{j+1}(0) = \underset{\sim}{x}^j(0) - \underset{\sim}{H}^j(\Gamma^j)^{-1}\underset{\sim}{F}\left(\underset{\sim}{x}^j(0)\right), \quad j = n,n+1,n+2,... \tag{32}$$

where

$$\underset{\sim}{F}\left(\underset{\sim}{x}^j(0)\right) \triangleq \underset{\sim}{x}^j(0) - \underset{\sim}{x}^j(T) \tag{33}$$

Equation (32) is precisely the n-dimensional secant method derived in Eq. (26), p. 197 of [14]. The convergence property of the secant method can be found in [14-15] and need not be repeated here. Observe that to initialize the secant method, we need "n+1" initial points $\underset{\sim}{x}^0(0)$, $\underset{\sim}{x}^1(0)$, $\underset{\sim}{x}^2(0),\ldots,\underset{\sim}{x}^n(0)$ in order to evaluate $\underset{\sim}{H}^n$ and $\underset{\sim}{\Gamma}^n$ from (29) and (30). Since $\underset{\sim}{x}^m(0) \triangleq \underset{\sim}{x}(mT)$, m = 0,1,2,...,n, these initial states can be obtained by solving (1) over the time interval $[0,(n+1)T]$. Now to compute $\underset{\sim}{F}\left(\underset{\sim}{x}^n(0)\right) \triangleq \underset{\sim}{x}^n(0) - \underset{\sim}{x}^n(T)$, we need to evaluate $\underset{\sim}{x}^n(T)$ which is obtained by solving (1) over [0,T] with $\underset{\sim}{x}^n(0)$ as the initial condition. In general, to compute $\underset{\sim}{F}\left(\underset{\sim}{x}^j(0)\right)$, we must evaluate $\underset{\sim}{x}^j(T)$ by solving (1) over [0,T] with $\underset{\sim}{x}^j(0)$ as the initial condition, j = n, n+1, n+2, ... Hence, after the initialization step which involves solving (1) over [0,(n+1)T], each iteration in the secant method requires that we solve (1) over [0,T] only once, as compared to n+1 times in the discretized Newton iteration.

One drawback of the secant method is that it could become unstable when one or more components of $\underset{\sim}{x}^{j-m}(0)$ are close to the exact solution $\hat{\underset{\sim}{x}}(0)$ for all m = 0,1,2,...,n. For example, suppose $x_k^{j-m}(0) \approx \hat{x}_k(0)$, m = 0,1,2,...,n, then the ratio of the round-off error in $F_k\left(\underset{\sim}{x}^{j-m}(0)\right) = x_k^{j-m}(0)-x_k^{j-m}(T)$ will become large for all m = 0,1,2,...,n. Now suppose the number of significant figures of the computer being used is p, and suppose

$$10^{-q} < \frac{|F_k\left(x^{j-m}(0)\right)|}{|x_k^{j-m}(0)|} = \frac{|x_k^{j-m}(0)-x_k^{j-m}(T)|}{|x_k^{j-m}(0)|} < 10^{-(q-1)} \tag{34}$$

then the number of significant figures of $F_k\left(\underset{\sim}{x}^{j-m}(0)\right)$ will be given by $s \leq p-q$. Consequently, the computer evaluation of $(\underset{\sim}{\Gamma}^j)^{-1}$ in (31) will result in large errors when s is small. Moreover, the accumulation of truncation error in the numerical integration of (1) will further reduce the number of significant figures when $x_k^{j-m}(0)$ is small. The preceding observation suggest that if

$$\left|\left[x_k^{j-m}(0)-x_k{}^{j-m}(T)\right] - \left[x_k^{j-m+1}(0)-x_k^{j-m+1}(T)\right]\right| < \varepsilon \tag{35}$$

for <u>all</u> m = 0,1,2,...,n and for sufficiently small ε, then $\underset{\sim}{\Gamma}^j$ will be ill-conditioned and the secant method will become unstable. To overcome this ill-conditioned situation, we propose that the secant method be modified so that (32) is applied only at those components satisfying the following <u>well-conditioned property</u>:

$$\left|F_k\left(\underset{\sim}{x}^{j-m}(0)\right) - F_k\left(\underset{\sim}{x}^{j-m+1}(0)\right)\right| \geq \varepsilon, \quad k = 1,2,\ldots,n \tag{36}$$

for <u>all</u> m = 0,1,2,...,n. For the remaining ill-conditioned components, we simply apply the <u>fixed-point algorithm</u> [10]. To implement this modified algorithm systematically, let us partition the components of $\underset{\sim}{x}^j(0)$ into two subvectors $\underset{\sim}{x}_\alpha^j(0)$ and $\underset{\sim}{x}_\beta^j(0)$ in accordance with the following rule: the <u>ith</u> component of $\underset{\sim}{x}^j(0)$ is assigned to the first subvector $\underset{\sim}{x}_\alpha^j(0)$ if $\gamma_i^j/\gamma_{max}^j \geq \delta$, where δ is a sufficiently small number,[5], and where γ_i^j and γ_{max}^j are obtained from the <u>ith</u> row of $\underset{\sim}{\Gamma}^j$:

$$\gamma_i^j \triangleq \left[\sum_{m=1}^{n}\left(\Gamma_{im}^j\right)^2\right]^{1/2} \tag{37}$$

$$\gamma_{max}^j \triangleq \max\{\gamma_1^j,\gamma_2^j,\ldots,\gamma_n^j\} \tag{38}$$

On the other hand, if $\gamma_i^j/\gamma_{max}^j < \delta$, then the <u>ith</u> component of $\underset{\sim}{x}^j(0)$ is assigned to the second subvector $\underset{\sim}{x}_\beta^j(0)$. The <u>modified secant algorithm</u> can now be summarized as follow:

---

[5]The choice of δ depends on the computer being used. Our experience shows that the secant method is always stable if we choose $\delta = 10^{-4}$ for a 16 bit computer and $\delta = 10^{-6}$ for a 32 bit computer.

Step 0. Choose an initial guess $\underset{\sim}{x}^0(0)$. Solve (1) for $\underset{\sim}{x}(t)$ with initial condition $\underset{\sim}{x}(0) = \underset{\sim}{x}^0(0)$ from t = 0 to t = (n+1)T. Set

$$\underset{\sim}{x}^k(0) = \underset{\sim}{x}^{k-1}(T) \triangleq \underset{\sim}{x}(kT), \quad k = 1,2,\ldots,n, \; n+1 \tag{39}$$

Step 1. Evaluate $\underset{\sim}{\Gamma}^j$ from (30) and compute γ_i^j and γ_{max}^j from (37) and (38), i = 1,2,...,n. Separate $\underset{\sim}{x}^j(0)$ into two subvectors $\underset{\sim}{x}_\alpha^j(0)$ and $\underset{\sim}{x}_\beta^j(0)$ using the preceding rule. Form the following:

$$\underset{\sim}{H}_\alpha^j \triangleq \left[\left(\underset{\sim}{x}_\alpha^{j-n}(0)-\underset{\sim}{x}_\alpha^{j-n+1}(0)\right)\left(\underset{\sim}{x}_\alpha^{j-n+1}(0)-\underset{\sim}{x}_\alpha^{j-n+2}(0)\right)\cdots\left(\underset{\sim}{x}_\alpha^{j-n+m-1}(0)-\underset{\sim}{x}_\alpha^{j-n+m}(0)\right)\right] \tag{40}$$

$$\underset{\sim}{\Gamma}_\alpha^j = \left[\left(\underset{\sim}{F}_\alpha\left(\underset{\sim}{x}^{j-n}(0)\right)-\underset{\sim}{F}_\alpha\left(\underset{\sim}{x}^{j-n+1}(0)\right)\right)\left(\underset{\sim}{F}_\alpha\left(\underset{\sim}{x}^{j-n+1}(0)\right)-\underset{\sim}{F}_\alpha\left(\underset{\sim}{x}^{j-n+2}(0)\right)\right)\cdots\left(\underset{\sim}{F}_\alpha\left(\underset{\sim}{x}^{j-n+m-1}(0)-\underset{\sim}{F}_\alpha\,\underset{\sim}{x}^{j-n+m}(0)\right)\right)\right] \tag{41}$$

where m is the number of variables contained in $\underset{\sim}{x}_\alpha^j$, and

$$\underset{\sim}{F}_\alpha\left(\underset{\sim}{x}^k(0)\right) \triangleq \underset{\sim}{x}_\alpha^k(0) - \underset{\sim}{x}_\alpha^k(T) \tag{42}$$

Step 2. Compute the components of $\underset{\sim}{x}^{j+1}(0)$ as follow:

$$\underset{\sim}{x}_\alpha^{j+1}(0) = \underset{\sim}{x}_\alpha^j(0) - \underset{\sim}{H}_\alpha^j(\underset{\sim}{\Gamma}_\alpha^j)^{-1}\underset{\sim}{F}_\alpha\left(\underset{\sim}{x}^j(0)\right) \qquad \text{(Secant algorithm)} \tag{43}$$

$$\underset{\sim}{x}_\beta^{j+1}(0) = \underset{\sim}{x}_\beta^j(T) \qquad \text{(Fixed-point algorithm)} \tag{44}$$

j = n, n+1, n+2, ...

Step 3. Compute $\underset{\sim}{x}^{j+1}(T)$ with $\underset{\sim}{x}^{j+1}(0)$ as initial condition. Go to Step 4 if $\|\underset{\sim}{x}^{j+1}(0)-\underset{\sim}{x}^{j+1}(T)\| < \varepsilon$ for some sufficiently small preassigned positive constant ε. Otherwise, set j = j+1 and go to Step 1.

Step 4. Stop.

B. Autonomous System

For autonomous systems having a T-periodic solution (1) assumes the form

$$\underset{\sim}{f}(\dot{\underset{\sim}{x}},\underset{\sim}{x},\underset{\sim}{y}) = \underset{\sim}{0} \tag{45}$$

where the period T must be determined along with the solution $\underset{\sim}{x}(t)$. This additional unknown variable can be accomodated in [2,10] by choosing some component of $\underset{\sim}{x}(t)$, say $x_p(t)$, and a constant C such that

$$\inf x_p(t) \leq C \leq \sup x_p(t) \tag{46}$$

Since the system is autonomous, we can choose the time origin such that $x_p(0) = C$. If $x_p(t)$ is T-periodic, we must also have $x_p(T) = C$, as illustrated

in Fig. 2. Hence in place of the initial value $x_p(0)$, which is now known, we insert T as the new variable to be determined. If we define

$$\underset{\sim}{z}(t) \triangleq \left[x_1(t)\ x_2(t),\ \ldots\ x_{p-1}(t)\ T(t)\ x_{p+1}(t)\ \ldots\ x_n(t)\right]^T \tag{47}$$

where T(t) is evaluated at $x_p(t) = C$, and is constant over $0 < t < T$, then our objective is to solve

$$\boxed{\underset{\sim}{F}\left(\underset{\sim}{z}(0)\right) \triangleq \underset{\sim}{z}(0) - \underset{\sim}{z}(T) = \underset{\sim}{0}} \tag{48}$$

To solve (48) via the secant method, let us assume the system of n vectors

$$\underset{\sim}{F}\left(\underset{\sim}{z}^j(0)\right) - \underset{\sim}{F}\left(\underset{\sim}{z}^{j+1}(0)\right) \triangleq \left[\left(\underset{\sim}{z}^j(0) - \underset{\sim}{z}^j(T^j)\right) - \left(\underset{\sim}{z}^{j+1}(0) - \underset{\sim}{z}^{j+1}(T^{j+1})\right)\right], \tag{49}$$

$j = m, m+1, \ldots, m+n$ for any $m \geq 0$ are linearly independent, and

$$\underset{\sim}{H}^j \triangleq \left[\left(\underset{\sim}{z}^{j-n}(0) - \underset{\sim}{z}^{j-n+1}(0)\right)\left(\underset{\sim}{z}^{j-n+1}(0) - \underset{\sim}{z}^{j-n+2}(0)\right)\cdots\left(\underset{\sim}{z}^{j-1}(0) - \underset{\sim}{z}^{j}(0)\right)\right] \tag{50}$$

$$\underset{\sim}{\Gamma}^j \triangleq \left[\left[\underset{\sim}{F}\left(\underset{\sim}{z}^{j-n}(0)\right) - \underset{\sim}{F}\left(\underset{\sim}{z}^{j-n+1}(0)\right)\right]\left[\underset{\sim}{F}\left(\underset{\sim}{z}^{j-n+1}(0)\right) - \underset{\sim}{F}\left(\underset{\sim}{z}^{j-n+2}(0)\right)\right]\cdots\left[\underset{\sim}{F}\left(\underset{\sim}{z}^{j-1}(0)\right) - \underset{\sim}{F}\left(\underset{\sim}{z}^{j}(0)\right)\right]\right] \tag{51}$$

then $\underset{\sim}{\Gamma}^j$ is <u>non-singular</u>, and the secant algorithm in this case assumes the form

$$\boxed{\underset{\sim}{z}^{j+1}(0) = \underset{\sim}{z}^j(0) - \underset{\sim}{H}^j(\underset{\sim}{\Gamma}^j)^{-1}\underset{\sim}{F}\left(\underset{\sim}{z}^j(0)\right)\ ,\quad j = n, n+1, \ldots} \tag{52}$$

where

$$\underset{\sim}{F}\left(\underset{\sim}{z}^j(0)\right) \triangleq \underset{\sim}{z}^j(0) - \underset{\sim}{z}^j(T_j) \tag{53}$$

Just as in the non-autonomous case, we need "n+1" initial points $\underset{\sim}{z}^0(0)$, $\underset{\sim}{z}^1(0)$, $\ldots,\underset{\sim}{z}^n(0)$ in order to evaluate (50) and (51). We define $\underset{\sim}{z}^m(0) \triangleq \underset{\sim}{z}^{m-1}(T_{m-1})$, $m = 1,2,\ldots,n+1$ where $\underset{\sim}{z}^{m-1}(T_{m-1})$ is obtained by solving (45) via BDF with $\underset{\sim}{z}(0) = \underset{\sim}{z}^{m-1}(0)$, and $x_p(0) = C$ as the initial value. Thus the initial states for determining $\underset{\sim}{H}^n, \underset{\sim}{\Gamma}^n$ can be obtained by solving (45) over the time interval $[0, T_0+T_1+\ldots+T_n]$. To determine the period T_m, let us choose a <u>kth</u> order (BDF) formula to solve (45) so that $x_p(t)$ can be extracted. This implies that the solution curve $x_p(t)$ is approximated by a <u>kth</u> degree polynomial

$$x_p(t) = a_0 + a_1 t + a_2 t^2 + \ldots + a_k t^k \tag{54}$$

where the coefficients $a_0, a_1, a_2, \ldots, a_k$ are determined by forcing $x_p(t)$ to

pass through k+1 points $x_p^n, x_p^{n-1}, \ldots, x_p^{n-k}$ at $t = t_n, t_{n-1}, \ldots, t_{n-k}$ [10]. This is equivalent to solving the following system of linear equations:

$$\begin{bmatrix} 1 & t_n & t_n^2 & \cdots & t_n^k \\ 1 & t_{n-1} & t_{n-1}^2 & \cdots & t_{n-1}^k \\ \cdot & \cdot & \cdot & \cdots & \cdot \\ \cdot & \cdot & \cdot & \cdots & \cdot \\ 1 & t_{n-k} & t_{n-k}^2 & \cdots & t_{n-k}^k \end{bmatrix} \begin{bmatrix} a_0 \\ a_1 \\ \cdot \\ \cdot \\ a_k \end{bmatrix} = \begin{bmatrix} x_p^n \\ x_p^{n-1} \\ \cdot \\ \cdot \\ x_p^{n-k} \end{bmatrix} \tag{55}$$

Hence, the period T_m can be obtained by solving (54) for $x_p = C$ via the Newton-Raphson method; namely,

$$\boxed{\begin{aligned} &f(t) \triangleq C - a_o - a_1 t - a_2 t^2 - \ldots\ldots - a_k t^k = 0 \\ &t^{j+1} = t^j - \frac{f(t^j)}{f'(t^j)} \quad , j = 0, 1, 2, \ldots\ldots \end{aligned}} \tag{56}$$

Since we can compute for all quantities needed in (52) and (53), the secant algorithm can also be implemented for autonomous systems. The only difference from the algorithm for the non-autonomous case is in <u>step 0</u>. Here, we set the <u>pth</u> component of $\underset{\sim}{x}(0)$ to C; namely, $x_p(0) = C$ and solve (45) via BDF from $t = 0$ to $t = T_0 + T_1 + \ldots + T_n$ and obtain $\underset{\sim}{z}^0(0), \underset{\sim}{z}^1(0), \ldots, \underset{\sim}{z}^n(0)$, as well as $\underset{\sim}{z}^0(T_0), \underset{\sim}{z}^1(T_1), \ldots, \underset{\sim}{z}^n(T_n)$. After this initialization step, the other steps are exactly the same as before. Again, to avoid ill-conditioned situations, the <u>modified secant algorithm</u> should be adopted for the autonomous case.

C. <u>Convergence Behavior of the Secant Method</u>

Our objective in this section is to analyze the convergence behavior of the secant method when applied to the equation

$$\underset{\sim}{F}\left(\underset{\sim}{x}(0)\right) \triangleq \underset{\sim}{x}(0) - \underset{\sim}{x}\left(T;\underset{\sim}{x}(0)\right) = \underset{\sim}{0} \tag{57}$$

without loss of generality, we can assume $\underset{\sim}{x}(0) = \underset{\sim}{0}$ is a solution of (57). Applying Taylor's expansion to each component of $\underset{\sim}{F}(\cdot)$ about $\underset{\sim}{x}(0) = \underset{\sim}{0}$, we obtain

$$F_i\left(\underset{\sim}{x}(0)\right) = \sum_{k=1}^{n}\left[F_{ik}x_k(0) + \frac{1}{2!}\sum_{m=1}^{n} F_{i,km}x_k(0)x_m(0) + \ldots\right] = 0 \tag{58}$$

$i = 1,2,\ldots,n$, where

$$F_{ik} \triangleq \left.\frac{\partial F_i\left(\underset{\sim}{x}(0)\right)}{\partial x_k(0)}\right|_{\underset{\sim}{x}(0)=\underset{\sim}{0}}, \quad F_{i,km} \triangleq \left.\frac{\partial^2 F_i\left(\underset{\sim}{x}(0)\right)}{\partial x_k(0)\partial x_m(0)}\right|_{\underset{\sim}{x}(0)=\underset{\sim}{0}} \tag{59}$$

Now assuming the Jacobian matrix $\partial\underset{\sim}{F}/\partial\underset{\sim}{x}(0)$ has n linearly independent eigenvectors, we can introduce a linear transformation

$$\underset{\sim}{u}(0) \triangleq \underset{\sim}{P}\underset{\sim}{x}(0) \tag{60}$$

which diagonalizes the Jacobian matrix so that (58) is transformed into the equivalent system

$$\boxed{\hat{F}_i\left(\underset{\sim}{u}(0)\right) = u_i(0) + \sum_{k=1}^{n}\sum_{m=1}^{n} B_{i,km}u_k(0)u_m(0) = 0 \qquad i = 1,2,\ldots,n.} \tag{61}$$

where all higher order terms in $\underset{\sim}{u}(0)$ have been neglected. We will analyze the convergence behavior of the secant method with respect to this equivalent system of n equations. The following property is proved in the Appendix 2:

Secant Method Convergence Lemma

If we apply the secant method to solve (61), then there exists a constant B_S such that[6]

$$\|\underset{\sim}{u}^{j+1}(0)\| = B_S\|\underset{\sim}{u}^{j-n}(0)\|\cdot\|\underset{\sim}{u}^{j}(0)\| \qquad \text{(Secant method)} \tag{62}$$

The corresponding property for Newton's method is given by [14]:

$$\|\underset{\sim}{u}^{j+1}(0)\| = B_N\|\underset{\sim}{u}^{j}(0)\|^2 \qquad \text{(Newton method)} \tag{63}$$

where B_N is a constant.[6] To compare the rate of convergence between the secant and Newton's method, let us take the natural log of both sides of (62) and (63):

$$\log\|\underset{\sim}{u}^{j+1}(0)\| = \log B_S + \log\|\underset{\sim}{u}^{j-n}(0)\| + \log\|\underset{\sim}{u}^{j}(0)\| \qquad \text{(Secant method)} \tag{64}$$

$$\log\|\underset{\sim}{u}^{j+1}(0)\| = \log B_N + 2\log\|\underset{\sim}{u}^{j}(0)\| \qquad \text{(Newton method)} \tag{65}$$

If we define

$$v_{S,m} \triangleq \log[B_S\|\underset{\sim}{u}^{m}(0)\|] = \log B_S + \log\|\underset{\sim}{u}^{m}(0)\| \qquad \text{(Secant method)} \tag{66}$$

$$v_{N,m} \triangleq \log[B_N\|\underset{\sim}{u}^{m}(0)\|] = \log B_N + \log\|\underset{\sim}{u}^{m}(0)\| \qquad \text{(Newton method)} \tag{67}$$

[6]Throughout this section, the subscript "S" pertains to the secant method, while the subscript "N" pertains to Newton's method.

then (64) and (65) can be recast into the following two linear difference equations:

$$v_{S,j+1} = v_{S,j-n} + v_{S,j} \qquad \text{(Secant method)} \qquad (68)$$

$$v_{N,j+1} = 2v_{N,j} \qquad \text{(Newton method)} \qquad (69)$$

The characteristic equations associated with (68) and (69) are therefore given by:

$$z_S^{n+1} - z_S^n - 1 = 0 \qquad \text{(Secant method)} \qquad (70)$$

$$z_N = 2 \qquad \text{(Newton's method)} \qquad (71)$$

For each n, the characteristic root $z_{S,n}$ of (70) can be easily computed. The solutions of the difference equations (68) and (69) are therefore given by $(v_{S,j} = z_{S,n}^j v_{S,0}$, $v_{N,j} = z_{N,n}^j v_{N,0})$:

$$\log[B_S \|\underset{\sim}{u}^j(0)\|] = z_{S,n}^j \log[B_S \|\underset{\sim}{u}^0(0)\|] \qquad \text{(Secant method)} \qquad (72)$$

$$\log[B_N \|\underset{\sim}{u}^j(0)\|] = 2^j \log[B_N \|\underset{\sim}{u}^0(0)\|] \qquad \text{(Newton method)} \qquad (73)$$

It follows from (72) and (73) that

$$\|\underset{\sim}{u}^j(0)\| = \frac{\exp\left[z_{S,n}^j \log\left(B_S \|\underset{\sim}{u}^0(0)\|\right)\right]}{B_S} = B_S^{z_{S,n}^j - 1} \|\underset{\sim}{u}^0(0)\|^{z_{S,n}^j} \qquad (74)$$

$$\|\underset{\sim}{u}^j(0)\| = \frac{\exp\left[2^j \log\left(B_N \|\underset{\sim}{u}^0(0)\|\right)\right]}{B_N} = B_N^{2^j - 1} \|\underset{\sim}{u}^0(0)\|^{2^j} \qquad (75)$$

Since B_S and B_N do not depend on j, the relationship between $\|\underset{\sim}{u}^{j+1}(0)\|$ and $\|\underset{\sim}{u}^j(0)\|$ is the same as that between $\|\underset{\sim}{u}^1(0)\|$ and $\|\underset{\sim}{u}^0(0)\|$. It follows from (74) and (75) that

$$\|\underset{\sim}{u}^{j+1}(0)\| = B_S^{z_{S,n} - 1} \|\underset{\sim}{u}^j(0)\|^{z_{S,n}} \qquad \text{(Secant method)} \qquad (76)$$

$$\|\underset{\sim}{u}^{j+1}(0)\| = B_N \|\underset{\sim}{u}^j(0)\|^2 \qquad \text{(Newton method)} \qquad (77)$$

Now since most of the time spent in solving (61) either by the secant or Newton method is used in solving (1) over one period, a more meaningful comparison between their respective convergence rates should take into account the number of times (1) has to be solved per iteration. If we disregard the initialization

step, then the secant method requires only one solution as compared to n+1 solutions in the Newton method. Hence, it is reasonable to define the respective convergence rates as follow:

$$t_S \triangleq z_{S,n} \qquad \text{(Secant method)} \tag{78}$$

$$t_N \triangleq 2^{1/(n+1)} \qquad \text{(Newton method)} \tag{79}$$

The value of t_S and t_N for different values of n can be easily computed and is listed in the first two columns of Table 1. Notice that the convergence rate of

Table 1. Comparison of convergence rates and computational efficiencies between the secant method and the Newton method.

n	t_s	t_N	I_s	I_N	R
1	1.618	1.414	7.218	8.634	1.196
2	1.466	1.259	9.822	12.951	1.318
3	1.380	1.189	12.290	17.268	1.405
4	1.325	1.149	14.632	21.585	1.475
5	1.285	1.122	15.932	25.902	1.626
10	1.184	1.065	27.716	47.487	1.713
20	1.114	1.034	47.716	90.657	1.900
50	1.058	1.014	103.071	220.167	2.136
100	1.034	1.007	189.497	436.017	2.301

the secant method is always greater than that of the Newton method.

Since the computation time for obtaining the periodic solution in either method is proportional to the total member "I" of transient analyses (i.e. solution of (1) over [0,T]) needed to reduce the error from the initial guess $\|\underset{\sim}{u}^0(0)\|$ to $\|\underset{\sim}{u}^j(0)\| = \varepsilon$, where ε is some prescribed number, a more meaningful comparison should be based on "I". Observe that since $\underset{\sim}{x}(0) = \underset{\sim}{0}$ is the exact solution (by assumption), $\varepsilon \to 0$ as $j \to \infty$. Now let $j = J_S(\varepsilon)$ and $j = J_N(\varepsilon)$ be the number of iterations required by the secant method and the Newton method, respectively, for $\|\underset{\sim}{u}(0)\|$ to decrease to some prescribed error $\varepsilon > 0$. We can estimate this number by setting $B_S = B_N = 1$ (for simplicity) in (72) and (73) and solve for $j \triangleq J_S(\varepsilon)$ and $j \triangleq J_N(\varepsilon)$ respectively:

$$J_S(\varepsilon) = \frac{\log\left[\log \varepsilon/\log\|\underset{\sim}{u}^0(0)\|\right]}{\log z_{S,n}} \qquad \text{(Secant method)} \qquad (80)$$

$$J_N(\varepsilon) = \frac{\log\left[\log \varepsilon/\log\|\underset{\sim}{u}^0(0)\|\right]}{\log 2} \qquad \text{(Newton method)} \qquad (81)$$

Since it takes "n" transient analysis over [0,T] to initiate the secant method, and since it takes one transient analysis per subsequent iteration, the total number I_S of transient analysis required by the secant method is given by

$$I_S = n + J_S(\varepsilon) \qquad \text{(Secant method)} \qquad (82)$$

where $J_S(\varepsilon)$ is defined by (80). Since each iteration in Newton's method requires n+1 transient analysis, the total number I_N of transient analysis required by Newton's method is given by

$$I_N = (n+1)J_N(\varepsilon) \qquad \text{(Newton method)} \qquad (83)$$

where $J_N(\varepsilon)$ is defined by (81). Clearly, I_S and I_N provide the most realistic comparison between the computational efficiencies of the two methods in so far as finding the periodic solutions of (1) is concerned. To obtain a numerical comparison, let us choose $\|\underset{\sim}{u}^0(0)\| = 0.5$ and $\varepsilon = 10^{-6}$. The corresponding number of transient analysis I_S and I_N required to reduce the error from 0.5 to 10^{-6} is computed and listed in columns 3 and 4 of Table 1. The ratio $R \triangleq I_N/I_S$ is shown in the last column of this table. Observe that the secant method is always more efficient than Newton's method. Observe also that R-increases monotonically with n, and hence the secant method becomes more efficient as the number n of state variables increases. This confirms our intuition that the secant method is superior to Newton's method especially for large-scale systems.

IV. A GLOBALLY CONVERGENT ALGORITHM FOR OBTAINING MULTIPLE PERIODIC SOLUTIONS

Both the Newton and the secant method require finding a suitable initial guess $\underset{\sim}{x}^0(0)$ in order to guarantee convergence. This is usually chosen in practice by intuition, experience (some prior knowledge of where the ballpark is), or trial and error. For unfamiliar systems, such initial guesses are difficult to find. For nonlinear systems having multiple periodic solutions, even a trial

and error method could not be used to find multiple initial solution points. Our objective in this section is to present a globally convergent algorithm which, under rather mild assumptions, is guaranteed to converge no matter what the initial guess is. Moreover, if the system has multiple periodic solutions, this algorithm will find most, if not all, of them.

The first step in this globally convergent algorithm is to augment the function $\underset{\sim}{F}\left(\underset{\sim}{x}(0)\right)$ in (57) with a parameter ρ, thereby transforming (57) into a new system

$$\boxed{\hat{\underset{\sim}{F}}\left(\underset{\sim}{x}(0),\rho\right) = \underset{\sim}{0}} \tag{84}$$

where $\hat{\underset{\sim}{F}}: \mathbb{R}^{n+1} \to \mathbb{R}^{n}$, and where $\hat{\underset{\sim}{F}}\left(\underset{\sim}{x}(0),\rho^*\right) \equiv \underset{\sim}{F}\left(\underset{\sim}{x}(0)\right)$ at some value $\rho = \rho^*$. There are many ways to construct $\hat{\underset{\sim}{F}}(\cdot)$. In many practical problems, the parameter ρ is already built in, as in the van der Pol equation [6], where $\rho \triangleq \mu$. In the absence of a natural parameter, we can introduce an artificial parameter ρ via the following "transformed equation":

$$\hat{\underset{\sim}{F}}\left(\underset{\sim}{x}(0),\rho\right) \triangleq \underset{\sim}{F}\left(\underset{\sim}{x}(0)\right) + (\rho-1)\ \underset{\sim}{F}\left(\underset{\sim}{x}^{0}(0)\right) = \underset{\sim}{0} \tag{85}$$

where $\underset{\sim}{F}\left(\underset{\sim}{x}(0)\right)$ is as defined in (57), and where $\underset{\sim}{x}^{0}(0)$ is an arbitrary initial guess. Now observe that at $\rho = 0$, (85) reduces to

$$\hat{\underset{\sim}{F}}\left(\underset{\sim}{x}(0),0\right) = \underset{\sim}{F}\left(\underset{\sim}{x}(0)\right) - \underset{\sim}{F}\left(\underset{\sim}{x}^{0}(0)\right) = \underset{\sim}{0} \tag{86}$$

Since $\underset{\sim}{x}(0) = \underset{\sim}{x}^{0}(0)$ is a solution of (86), it is clear that $\underset{\sim}{x}^{0}(0)$ will be a good initial guess for solving (85) by either Newton or secant method for small values of ρ. The basic idea behind the algorithm to be presented next is to find an efficient way to continue this solution as ρ increases continuously. Since (84) reverts to (57) when $\rho = \rho^* = 1$, the exact solution we seek occurs at $\rho = 1$. Since this algorithm is a direct application of the switching parameter approach, the reader is referred to [12] for the details of the derivation. Here, we will simply describe the switching-parameter algorithm as applied to the problem of this paper.

The algorithm consists of two basic steps. First, we predict $\underset{\sim}{x}^{j+1}(0)$ and ρ^{j+1} via the forward Euler algorithm. Then we reduce the local truncation error using the secant method. The geometrical interpretation of this algorithm for the $n = 1$ case is shown in Fig. 3. Here, the algorithm traces a continuous

"solution curve" Γ in the $x(0)$ - vs. - ρ plane, starting from $x(0) = x^0(0)$ and $\rho = 0$. The solution occurs at the intersection of this curve with the vertical line $\rho = \rho^*$, where $\rho^* = 1$ if (85) is chosen. The forward Euler method generates the points at the tip of the arrowheads while the secant method corrects the error by moving each of these points either vertically, or horizontally, back into Γ. A vertical (resp., horizontal) movement occurs when the vertical increment (due to the step size h) as computed by the forward Euler algorithm is <u>less than</u> (resp., <u>more than</u>) h and corresponds to the choice of ρ (resp., $x(0)$) as the <u>independent variable</u> defining the solution curve Γ. Observe that this variable could switch back and forth between ρ and $x(0)$ many times, depending on the nature of Γ, hence the name <u>switching parameter algorithm</u>. The two steps of this algorithm are:

<u>Step 1</u>.

Predictor algorithm by Forward Euler method

$$\underset{\sim}{J}\left(\underset{\sim}{x}^j(0), \rho^j\right)\begin{bmatrix} \underset{\sim}{x}^{j+1}(0) - \underset{\sim}{x}^j(0) \\ \rho^{j+1} - \rho^j \end{bmatrix} = -\hat{\underset{\sim}{F}}\left(\underset{\sim}{x}^j(0), \rho^j\right) \tag{87}$$

$$\operatorname{sgn}\left[x_k^j(0) - x_k^{j-1}(0)\right]\left[x_k^{j+1}(0) - x_k^j(0)\right] = h$$

where

$$\underset{\sim}{J}\left(\underset{\sim}{x}(0), \rho\right) \triangleq \left[\begin{array}{cccc|c} \frac{\partial \hat{F}_1\left(\underset{\sim}{x}(0),\rho\right)}{\partial x_1(0)} & \frac{\hat{F}_1\left(\underset{\sim}{x}(0),\rho\right)}{\partial x_2(0)} & \cdots & \frac{\partial \hat{F}_1\left(\underset{\sim}{x}(0),\rho\right)}{\partial x_n(0)} & \frac{\partial \hat{F}_1\left(\underset{\sim}{x}(0),\rho\right)}{\partial \rho} \\ \frac{\partial \hat{F}_2\left(\underset{\sim}{x}(0),\rho\right)}{\partial x_1(0)} & \frac{\partial \hat{F}_2\left(\underset{\sim}{x}(0),\rho\right)}{\partial x_2(0)} & \cdots & \frac{\partial \hat{F}_2\left(\underset{\sim}{x}(0),\rho\right)}{\partial x_n(0)} & \frac{\partial \hat{F}_2\left(\underset{\sim}{x}(0),\rho\right)}{\partial \rho} \\ \vdots & \vdots & \cdots & \vdots & \vdots \\ \frac{\partial \hat{F}_n\left(\underset{\sim}{x}(0),\rho\right)}{\partial x_1(0)} & \frac{\partial \hat{F}_n\left(\underset{\sim}{x}(0),\rho\right)}{\partial x_2(0)} & \cdots & \frac{\partial \hat{F}_n\left(\underset{\sim}{x}(0),\rho\right)}{\partial x_n(0)} & \frac{\partial \hat{F}_n\left(\underset{\sim}{x}(0),\rho\right)}{\partial \rho} \end{array}\right] = \left[\frac{\partial \hat{\underset{\sim}{F}}\left(\underset{\sim}{x}(0),\rho\right)}{\partial \underset{\sim}{x}(0)} \;\Big|\; \frac{\partial \hat{\underset{\sim}{F}}\left(\underset{\sim}{x}(0),\rho\right)}{\partial \rho}\right] \tag{88}$$

The kth component $x_k(0)$ in (87) corresponds to the component of $\underset{\sim}{x}(0)$ having the <u>maximum</u> variation; namely,

$$|\Delta x_k^{j+1}| \triangleq |x_k^j(0) - x_k^{j-1}(0)| = \max\left\{|\Delta x_1^j|, |\Delta x_2^j|, \ldots\ldots, |\Delta x_n^j(0)|, |\Delta \rho^j|\right\} \tag{89}$$

where $\Delta x_i^j \triangleq x_i^j(0) - x_i^{j-1}(0), \quad i = 1, 2, 3, \ldots\ldots, n$

$\Delta \rho \triangleq \rho^j - \rho^{j-1}$

It follows from (89) that the maximum variation at the jth step is equal or less than h. The second equation in (87) guarantees that the solution curve Γ is traced in the same direction of $x_k(0)$ at the (j-1)th step.

Step 2. The predicted value from (87) is corrected by the following algorithm:

Corrector algorithm by secant method

$$\underset{\sim}{J}\left(\underset{\sim}{x}^i(0),\rho^i\right)\begin{bmatrix}\underset{\sim}{x}^{i+1}(0) - \underset{\sim}{x}^i(0)\\ \rho^{i+1} - \rho^i\end{bmatrix} = -\hat{\underset{\sim}{F}}\left(\underset{\sim}{x}^i(0),\rho^i\right) \tag{90}$$

$$x_k^{i+1}(0) = x_k^i(0)$$

where $i = j+1$

Observe that the first submatrix $\partial\hat{\underset{\sim}{F}}\left(\underset{\sim}{x}(0),\rho\right)/\partial\underset{\sim}{x}(0)$ in (88) can be obtained by the secant method via (31):

$$\frac{\partial\hat{\underset{\sim}{F}}\left(\underset{\sim}{x}^j(0),\rho^j\right)}{\partial\underset{\sim}{x}^j(0)} = (\underset{\sim}{\Gamma}^j)(\underset{\sim}{H}^j)^{-1} \tag{91}$$

where $\hat{\underset{\sim}{F}}\left(\underset{\sim}{x}^m(0),\rho^m\right) = \underset{\sim}{x}^m(0) - \underset{\sim}{x}^m(T)$

and $$\underset{\sim}{\Gamma}^j \triangleq \left[\left[\hat{\underset{\sim}{F}}\left(\underset{\sim}{x}^{j-n}(0),\rho^{j-n}\right) - \hat{\underset{\sim}{F}}\left(\underset{\sim}{x}^{j-n+1}(0),\rho^{j-n+1}\right)\right]\left[\hat{\underset{\sim}{F}}\left(\underset{\sim}{x}^{j-n+1}(0),\rho^{j-n+1}\right) - \hat{\underset{\sim}{F}}\left(\underset{\sim}{x}^{j-n+2}(0),\rho^{j-n+2}\right)\right] \ldots\ldots \left[\hat{\underset{\sim}{F}}\left(\underset{\sim}{x}^{j-1}(0),\rho^{j-1}\right) - \hat{\underset{\sim}{F}}\left(\underset{\sim}{x}^{j}(0),\rho^{j}\right)\right]\right] \tag{92}$$

$$\underset{\sim}{H}^j \triangleq \left[\left(\underset{\sim}{x}^{j-n}(0) - \underset{\sim}{x}^{j-n+1}(0)\right)\left(\underset{\sim}{x}^{j-n+1}(0) - \underset{\sim}{x}^{j-n+2}(0)\right)\ldots\left(\underset{\sim}{x}^{j-1}(0) - \underset{\sim}{x}^{j}(0)\right)\right] \tag{93}$$

The second submatrix can be obtained as follow:

$$\frac{\partial\hat{\underset{\sim}{F}}\left(\underset{\sim}{x}(0),\rho\right)}{\partial\rho} = \frac{\hat{\underset{\sim}{F}}\left(\underset{\sim}{x}(0),\rho+\Delta\rho\right) - \hat{\underset{\sim}{F}}\left(\underset{\sim}{x}(0),\rho\right)}{\Delta\rho} \quad ; \text{ for augmented system (84).} \tag{94}$$

$$= \hat{\underset{\sim}{F}}\left(\underset{\sim}{x}^0(0)\right) \quad ; \text{ for augmented system (85).} \tag{95}$$

where $\Delta\rho$ in (94) is chosen to be a small number. It is proved in [12] that the solution curve Γ obtained by the above algorithm has the following two properties:

Property 1.

If the rank of the nx(n+1) matrix $\left[\partial\hat{\underset{\sim}{F}}\left(\underset{\sim}{x}(0),\rho\right)/\partial\underset{\sim}{x}(0) \vdots \partial\hat{\underset{\sim}{F}}\left(\underset{\sim}{x}(0),\rho\right)/\partial\rho\right]$ is equal to n along the solution curve of (84), then, the predictor algorithm (87) always

gives a unique solution $\left(\underset{\sim}{x}^{j+1}(0),\rho^{j+1}\right)$.

Property 2.

Let $\underset{\sim}{x}_o'(0)$ and $\underset{\sim}{x}_o''(0)$ be any two initial points which are independent in the sense that $\underset{\sim}{F}\left(\underset{\sim}{x}_o'(0)\right) \neq k\underset{\sim}{F}\left(\underset{\sim}{x}_o''(0)\right)$, where k is an arbitrary constant. Let $\Gamma\left(\underset{\sim}{x}_o'(0)\right)$ and $\Gamma\left(\underset{\sim}{x}_o''(0)\right)$ denote the respective solution curves plotted in the $\underset{\sim}{x}(0)$-space with ρ as a parameter. Then any intersection $\hat{\underset{\sim}{x}}(0)$ between $\Gamma\left(\underset{\sim}{x}_o'(0)\right)$ and $\Gamma\left(\underset{\sim}{x}_o''(0)\right)$ must necessarily be an initial point which gives rise to a steady-state periodic solution of (1).

Observe that Property 1 guarantees that our algorithm can indeed generate a solution curve Γ through any initial point $\underset{\sim}{x}^0(0)$ continuously. The value $\underset{\sim}{x}(0)$ corresponding to $\rho = \rho^*$ then gives the desired periodic solution. Since $\underset{\sim}{x}^0(0)$ can be arbitrarily chosen, our algorithm is indeed globally convergent under the mild assumption that $\rho = \rho^*$. Property 2 guarantees that if (1) has multiple periodic solutions, then by choosing two or more initial points, all intersections of the associated solution curves must correspond to periodic solutions. We can now summarize the above algorithm as follow:

Globally Convergent Algorithm

Step 0. Choose any initial value $\underset{\sim}{x}^0(0)$ and ρ^0. Choose the kth component x_k^0 to be ρ^0.[7]

Step 1. Compute $\underset{\sim}{\Gamma}^j$ and $\underset{\sim}{H}^j$ as defined in (92) and (93) by solving (1) over [0,T] n+1 times. Evaluate $\partial\hat{\underset{\sim}{F}}\left(\underset{\sim}{x}(0),\rho\right)/\partial\rho$ by (94) or (95). Hence $\underset{\sim}{J}\left(\underset{\sim}{x}^j(0),\rho^j\right)$ is determined.

Step 2. Implement the Predictor algorithm by solving (87) for $\underset{\sim}{x}^{j+1}(0)$ and ρ^{j+1} using the Gaussian elimination method.

Step 3. Find $|\Delta x_k^{j+1}|$ using (89).

If $|\Delta x_k^{j+1}| = |\Delta x_k^j|$, go to step 4.

If $|\Delta x_k^{j+1}| \neq |\Delta x_k^j|$, switch from the parameter $x_k^j(0)$ to the parameter $x_k^{j+1}(0)$ and go to step 4.

Step 4. Implement the corrector algorithm (90) for i = j+1 until $\|\hat{\underset{\sim}{F}}\left(\underset{\sim}{x}^{i+1}(0),\rho^{i+1}\right)\| < \varepsilon$ where ε is a sufficiently small positive constant.[8]

---

[7] Since initially there is yet no "variation" in $\underset{\sim}{x}^0(0)$, we can choose any variable as the kth component.

[8] The examples in the next section are all solved with $\varepsilon = 10^{-6}$.

Step 5.[9] If $\rho^j < \rho^*$, go to step 2 with $j = j+1$, $\underset{\sim}{x}^j(0) = \underset{\sim}{x}^{i+1}(0)$ and $\rho^j = \rho^{i+1}$. If $\rho^j \geq \rho^*$, go to step 6.

Step 6. Interpolate to identify the point $\hat{\underset{\sim}{x}}(0)$ where $\rho^j = \rho^*$. Then the solution of (1) through $\hat{\underset{\sim}{x}}(0)$ is T-periodic. Stop.

To obtain multiple periodic solutions, we simply repeat the above algorithm, and continue to trace the solution curve. The intersections between the different solution curves must all occur at exactly $\rho = \rho^*$, each of which gives rise to a distinct T-periodic solution. In the event where there is reason to believe that other T-periodic solutions remain unidentified, repeat the algorithm with other initial guesses. Except in rare cases, our experience shows that all periodic solutions will be found with no more than 4 initial guesses.

V. ILLUSTRATIVE EXAMPLES

Example 1. High-Q Bandpass Filter

Consider the high Q active bandpass filter circuit shown in Fig. 4(a) where the transistors are modelled by the "dc" Ebers-Moll model shown in Fig. 4(b). The diffusion and transition capacitances of the transistors are negligible for this filter which was designed to have a bandwidth extending from $\omega_1 = 980$ rad./sec. to $\omega_2 = 1020$ rad./sec. The following reduced system of implicit differential-algebraic equations for this network is obtained by the algorithm described in Appendix 1:

$$
\begin{aligned}
&G_1 v_{11} - C_1 \dot{v}_1 = 0 \\
&C_1 \dot{v}_1 - i_8 = 0 \\
&L_8 \dot{i}_8 + v_{in} + v_{11} + v_1 - v_2 = 0 \\
&C_2 \dot{v}_2 + i_8 + i_9 + i_{10} = 0 \\
&v_2 - L_9 \dot{i}_9 = 0 \\
&-i_{10} + C_4 \dot{v}_4 = 0 \\
&L_{10} \dot{i}_{10} - v_2 + v_3 + v_{12} + v_4 = 0 \\
&-C_4 \dot{v}_4 + (G_4 + G_2)(v_3 + v_{12}) - G_4 E_b + (1-\alpha)(I_{d11} + I_{d12}) = 0 \\
&G_3 v_3 + C_3 \dot{v}_3 + \alpha I_{d12} - I_{d11} = 0
\end{aligned}
\tag{96}
$$

[9] If the augmented system (85) is chosen, then $\rho^* = 1$.

$$
\begin{aligned}
&G_5(v_6+v_{13}+v_5-E_b)+C_6\dot{v}_6+\alpha I_{d11}-I_{d12} = 0\\
&-C_6\dot{v}_6+(G_8+G_6)(v_5+v_{13})-G_8E_b+(1-\alpha)(I_{d21}-I_{d22}) = 0\\
&G_7v_5+C_5\dot{v}_5+\alpha I_{d22}-I_{d21} = 0\\
&C_7\dot{v}_7+G_9(v_{14}+v_7-E_b)+\alpha I_{d21}-I_{d22} = 0\\
&-C_7\dot{v}_7+G_{10}v_{14} = 0
\end{aligned}
$$

Equation (96) consists of 14 equations with

$$\underset{\sim}{x} = [v_1v_2v_3v_4v_5v_6v_7i_8i_9i_{10}]^T \tag{97}$$

as the state variables; hence, n = 10. We use the 4th order backward differentiation formula (BDF) with a step size h = T/40 to solve (96). The initial guess $\underset{\sim}{x}(0)$ is chosen to be the following dc solution with $v_{in} = 0$ which can be obtained by BDF with a large step size (e.g., h = 100):

$$
\begin{aligned}
&v_1(0) = v_2(0) = 0,\ v_3(0) = 0.544,\ v_4(0) = -0.875,\ v_5(0) = 0.544,\ v_6(0) = 8.80,\\
&v_7(0) = 9.67,\ i_8(0) = i_9(0) = i_{10}(0) = 0,\ v_{11}(0) = 0,\ v_{12}(0) = 0.330,\\
&v_{13}(0) = 0.330,\ v_{14}(0) = -8.79
\end{aligned} \tag{98}
$$

the output voltage v_{out} which gives rise to a periodic solution is computed using the modified secant method in Section III for 3 different values of δ and the result is listed in Table 2.

Table 2. Steady-state analysis of bandpass filter via the modified secant method with δ as a parameter. ($v_{in}(t) = E_m \sin \omega t$, ω = 990 rad./sec., E_m = 0.01 volts).

I	δ = 0.01		δ = 0.0001		δ = 0	
	v_{out}	Error	v_{out}	Error	v_{out}	Error
1	2.6442	2.7369×10^{-2}	2.6442	3.7369×10^{-2}	2.6442	3.7369×10^{-2}
5	2.8220	4.6603×10^{-1}	2.6503	7.8222×10^{-1}	2.6503	7.8222×10^{-1}
9	2.6996	1.6381×10^{-1}	2.6603	4.3609×10^{-3}	2.6603	4.3609×10^{-3}
13	2.5445	1.9875×10^{-2}	2.6588	5.8248×10^{-4}	2.6588	5.8248×10^{-4}
15	2.6251	3.7291×10^{-1}	2.6584	2.4586×10^{-5}	2.6584	2.4586×10^{-5}
17	2.6898	4.2957×10^{-2}	2.6587	2.9987×10^{-4}	2.6586	6.9357×10^{-5}
18	2.9778	3.1342×10^{-1}	2.6585	6.9124×10^{-5}	2.6582	1.2515×10^{-3}
19	—	—	2.6585	7.1399×10^{-5}	2.6586	3.9048×10^{-4}

The error in Table 2 is defined by

$$\text{Error} \triangleq \left\{ \sum_{m=1}^{7} \left[v_m(0) - v_m(T) \right]^2 + \sum_{m=8}^{10} \left[i_m(0) - i_m(T) \right]^2 \right\}^{1/2} \tag{99}$$

Note that when $\delta = 0.01$, the error oscillates and the algorithm is unstable. However, with $\delta = 0.0001$ or $\delta = 0$, the algorithm converges in about 13 iterations. Our experience shows that the choice of δ depends strongly on the choice of the computer. For a 16 bit computer, our algorithm is found to be always stable with $\delta = 10^{-4}$ or 10^{-5}. For a 32 bit computer, even more accurate solution is obtained with $\delta = 10^{-8}$, as shown in Table 3. The same circuit is analyzed using the discretized Newton method from Section II and the solution is seen to converge in 5 iterations, as shown in Table 4. This rapid convergence is misleading

Table 3. Steady-state analysis of bandpass filter using modified secant method using a 32 bit computer. (ω = 990 rad./sec., E_m = 0.001 volts).

I	v_{out}	Error
1	0.42631	1.2148×10^{-2}
2	0.47041	7.5861×10^{-3}
3	0.47056	2.4694×10^{-3}
4	0.47058	2.4620×10^{-3}
5	0.47054	1.9284×10^{-3}
12	0.47054	1.9108×10^{-3}
13	0.47070	4.1449×10^{-7}
14	0.47071	2.8706×10^{-7}
15	0.47071	5.8717×10^{-7}

Table 4. Steady-state analysis of bandpass filter using discretized Newton method (ω = 990 rad./sec., E_m = 0.01 volts).

I	v_{out}	Error
1	2.8433	6.9272×10^{-1}
2	3.1518	1.3215×10^{-1}
3	2.7120	9.7060×10^{-2}
4	2.6588	2.9671×10^{-4}
5	2.6587	2.5867×10^{-4}

however, because each iteration in the modified secant method requires solving (96) over [0,T] only once, whereas that of Newton's methods, requires n+1 = 11 separate solutions. Hence a more meaningful comparison should be based on the number of times that the circuit has to be analyzed by BDF over [0,T] per iteration. Such a comparison has been made using 4 methods: 1) "brute force" transient analysis, 2) discretized Newton method, 3) secant method and, 4) modified secant method. The result is summarized in Fig. 5. Observe that the transient analysis method converges extremely slowly. This is expected since this filter has a very high Q (very lightly damped) and hence it takes a

long time before the transient will die out. In contrast to this, the discretized Newton iteration converges after 44 transient analyses, the secant method converges after 29 analyses, while the modified secant method requires only 23 analyses. Observe that the graph for the modified secant method coincides with that of the transient analysis method (which is equivalent to the fixed-point algorithm [10]) for $n \leq 11$ because the modified secant method must be initiated by "n+1" transient analyses. Observe also that the graph corresponding to the secant method in [15] is quite erratic in view of the ill-conditioned problem alluded to earlier. The computation time of the discretized Newton method is found to be about 1.8 times that of the modified secant method when ω = 990 rad./sec., and 1.3 when ω = 1020 rad./sec. This agrees quite well with the predicted ratio R = 1.713 in Table 1 for n = 10. At ω = 1040 rad./sec., the modified secant method is found to converge in 21 iterations while the discretized Newton method becomes unstable and does not converge at all.

Using the initial values found in the preceding analysis, the periodic steady state output waveforms $v_{out}(t)$ correspondong to two different input amplitudes E_m = 0.001 and 0.01 volts are shown in Fig. 6(a) for the input frequency ω = 990 rad./sec. The corresponding waveforms corresponding to E_m = 0.002 and 0.01 volts are shown in Fig. 6(b) for the input frequency ω = 1040 rad./sec. Notice that this waveform is much more distorted compared to that in Fig. 6(a). Since the initial guess in this case is quite far from the exact solution, it is not surprising that the discretized Newton method diverges.

Example 2. Modified Colpitt Sine and Cosine Oscillator

Consider next the autonomous circuit shown in Fig. 7(a), where the left hand side consists of a modified Colpitt's oscillator. This circuit is designed to generate a sine wave ($v_b(t)$ and $v_c(t)$) and a cosine wave ($v_a(t)$) simultaneously. The frequency is controlled by the inductor L_5. Using the same circuit model in Fig. 4(b) for the transistors, we obtain the following reduced system of implicit differential-algebraic equations:

$$
\begin{aligned}
&G_1(v_1-v_6)+G_2(v_1-v_6+E_b)+(\alpha-1)(I_{d11}+I_{d12}) = 0\\
&G_3(v_1+E_b)+I_{d11}-\alpha I_{d12}+C_2\dot{v}_2+C_1\dot{v}_1+i_5 = 0\\
&i_4-C_2\dot{v}_2+I_{d12}-\alpha I_{d11} = 0\\
&L_4\dot{i}_4+v_2-v_1 = 0\\
&-i_5+G_4(v_7-v_8+v_3-v_{10})+I_{d21}-\alpha I_{d22} = 0
\end{aligned}
\qquad (100)
$$

$$
\begin{aligned}
&-v_8+v_7-v_{10}+v_3+L_5\dot{i}_5-v_1-E_b = 0\\
&G_7(v_3-v_8-v_{10})+G_6(v_3-v_8-v_{10}-E_b)+(\alpha-1)(I_{d21}+I_{d22}) = 0\\
&G_5(-v_{10}+v_3-E_b)+C_3\dot{v}_3+I_{d22}-\alpha I_{d21} = 0\\
&-G_9v_{10}+G_8(-v_{10}-E_b)+(\alpha-1)(I_{d31}+I_{d32})-C_3\dot{v}_3 = 0\\
&G_{10}(-v_{10}+v_9)+I_{d31}-\alpha I_{d32} = 0
\end{aligned}
$$

The state variables are $\underset{\sim}{x} = [v_1 v_2 v_3 i_4 i_5]^T$ and hence, n = 5. We solve (100) using the 4th order BDF as in example 1, and use the modified secant method to find the periodic solution. Again, the dc solution is chosen as the initial guess $\underset{\sim}{x}^0(0)$. This solution is easily found using the BDF with a large step size h to guarantee that the algorithm will be stable, i.e., will lie in the shaded region of the stability diagram [10] shown in Fig. 8(a). The convergence behavior of the modified secant method is shown in Fig. 8(b) for 3 different values of R_6. Since n = 5, the first 6 periods of transient analysis in Fig. 8(b) correspond to the fixed-point algorithm $\underset{\sim}{x}^{j+1}(0) = \underset{\sim}{x}^j(T^{j+1})$. Since this circuit is autonomous, we have fix $v_1(0) = 9.12$ in all iterations and replace v_1 with the unknown period T; i.e., $\underset{\sim}{z} = [T v_2 v_3 i_4 i_5]^T$. We use (55) and (56) to calculate T and use BDF to calculate v_2, v_3, i_4 and i_5 in implementing the modified secant method. The results in Fig. 8(b) are all obtained with $\delta = 10^{-4}$. The output voltage waveforms $v_a(t)$, $v_b(t)$ and $v_c(t)$ corresponding to R = 450Ω are shown in Fig. 7(b), where $T = 0.58693 \times 10^{-3}$. The same waveforms for R = 430Ω are shown in Fig. 7(c), where $T = 0.58540 \times 10^{-3}$. Observe that the waveforms $v_b(t)$ and $v_c(t)$ are highly distorted because transistor T_2 is saturated when R = 430Ω.

Example 3. Nonlinear Frequency Response for Duffings's Equation

Consider the "forced" nonlinear series RLC resonant circuit shown in Fig. 9(a). The circuit equation

$$\ddot{x} + k\dot{x} + a_1 x + a_2 x^3 = B \sin \omega t \tag{101}$$

is known as Duffing's equation [6] and can be recast into the following state variable form:

$$
\left.
\begin{aligned}
\dot{x}_1 &= x_2\\
\dot{x}_2 &= -kx_2 - a_1 x_1 - a_2 x_1^3 + B \sin \omega t
\end{aligned}
\right\} \tag{102}
$$

We apply the discretized Newton method and the secant method to solve (102) with B = 5.0, k = 0, $a_1 = a_2 = 1.0$, and $\omega = 1.5$. The results are summarized in Table 7. In this case both methods converge rapidly even though there is

Table 7. Comparison of discretized Newton method and secant method.

I	Discretized Newton Method		Secant Method	
	$x_1(0)$	$x_2(0)$	$x_1(0)$	$x_2(0)$
1	0.32013E-01	0.21371E+01	-0.37333E-01	0.23598E+01
2	-0.18178E-02	0.24009E+01	-0.61868E-02	0.23839E+01
3	-0.13519E-03	0.23986E+01	-0.27407E-03	0.23983E+01
4	-0.13181E-03	0.23986E+01	-0.13123E-03	0.23986E+01
5	-0.13161E-03	0.23986E+01	-0.13177E-03	0.23986E+01

no damping. To obtain the same accuracy, we find that 9 iterations are required by the discretized Newton method compared to only 6 required by the secant method. Consequently, the secant method is more efficient even for small n.

It is well known that Duffing's equation exhibits many interesting nonlinear phenomena [6,16]. For example, it has multiple periodic solutions at around B = 0.4. It can also exhibit jump resonance and subharmonic oscillations. In this case, we introduce an artificial parameter ρ and choose the augmented system (85). Now assume B = 0.4, k = 0.1, $a_1 = a_2 = 1.0$, $\omega = 1.5$ and choose h = 0.05 as the step size for the forward Euler algorithm (87). Applying the globally convergent algorithm to this system, we obtain 4 solution curves $(x_1(t), x_2(t), \rho(t))$ corresponding to the following 4 initial guesses: P_1: (0,0) P_2: (-2,2) P_3: (-2,-2) P_4: (0,-2). These curves are projected into the $x_1(0)$ -vs.- $x_2(0)$ plane as shown in Fig. 9(b). Observe that these solution curves intersect at three points Q_1, Q_2, and Q_3, each one giving rise to a T-periodic solution. Observe that only solution curve 2 (corresponding to initial guess P_2 is sufficient to locate the three points Q_1, Q_2, and Q_3. The three associated T-periodic solutions corresponding to Q_1 and Q_3 are stable, while that corresponding to Q_2 is unstable.

Let us derive next the nonlinear frequency response curves as a function of the amplitude B of the input. In this case, it is natural to choose $\rho = B$ and work with the augmented system (84). Let us choose k = 0.4, $a_1 = 0$, $a_2 = 1.0$ and $\omega = 1$ and derive the solution curve starting from $(x_1(0), x_2(0), B) = (0,0,0)$ using the globally convergent algorithm. Since ρ coincides with B in

this case, each point on the solution curve determines a T-periodic solution, where $T = 2\pi$. If we find the Fourier components of each of these periodic solutions, we would obtain the family of frequency response curves, one for each harmonic component. Here, the dotted lines indicate the corresponding solutions are unstable, while the solid linesdenote stable solutions. We find the dc and 2nd harmonic components can occur only over the range $2.9219 \leq B \leq 11.922$. We also find that jump phenomena occur over the two intervals $0.44829 \leq B \leq 0.52323$ and $12.382 \leq B \leq 14.455$. These bounds are exact and could not have been obtained by any other existing methods known to the authors.

Since it is well-known that Duffing's equation can have a 1/3 subharmonic solution, let us derive the frequency response characteristics of this mode of oscillation as a function of B. To be specific, let us choose $k = 0.1$, $a_1 = 0$, $a_2 = 1.0$, and $\omega = 1$. Repeating the preceding procedure but with $3T = 6\pi$, we obtain the results shown in Figs. 10(a) for $0.10 \leq B \leq 0.25$, and in Fig. 10(b) for $1.3 \leq B \leq 1.7$. Again, observe that these characteristic curves are all exactly (apart from truncation errors) determined by our algorithm. The conventional methods for generating these curves make use of the harmonic balance method by neglecting higher harmonic terms which are invariably present. Consequently, all such characteristic curves are only approximately determined. Finally, Fig. 10(c) shows a pair of 1/3 order subharmonic response waveforms $x_1(t)$ and $x_2(t)$ corresponding to an input amplitude $B = 0.1581$. An examination of Fig. 10(a) shows that these waveforms contain only two component frequencies; namely, the input frequency ω and the 1/3 order subharmonic frequency $\omega/3$.

Example 1. van der Pol Oscillator

Consider next the autonomous nonlinear circuit shown in Fig. 11(a) where the tunnel diode i_D-v_D curve shown in Fig. 11(b) is described by

$$f(v_D) = -\rho_1(v-E) + \rho_3(v-E)^3, \quad \rho_1,\rho_3 > 0 \tag{103}$$

The circuit equation is given by

$$f(v+E) + Gv + C\frac{dv}{dt} + i_L = 0, \quad L\frac{di_L}{dt} = v \tag{104}$$

Substituting (103) into (104) and simplifying, we obtain

$$C\frac{d^2v}{dt^2} + (G-\rho_1+3\rho_3v^2)\frac{dv}{dt} + \frac{1}{L}v = 0 \tag{105}$$

Now introduce the dimensionless time variable $\tau = \frac{1}{\sqrt{LC}}\, t$ and recast (105) into the form

$$\frac{d^2v}{d\tau^2} + \sqrt{\frac{L}{C}}\,(\rho_1 - G)\left[-1 + \frac{3\rho_3}{\rho_1 - G}\, v^2\right]\frac{dv}{d\tau} + v = 0 \tag{106}$$

If we define

$$x \triangleq \frac{3\rho_3}{\rho_1 - G}\, v, \qquad \mu \triangleq \sqrt{\frac{L}{C}}\,(\rho_1 - G) \tag{107}$$

then (106) becomes the well-known van der Pol equation [6]:

$$\frac{d^2x}{d\tau^2} - \mu(1-x^2)\frac{dx}{d\tau} + x = 0 \tag{108}$$

In state variable form, (108) becomes

$$\begin{aligned} \dot{x}_1 &= x_2 \\ \dot{x}_2 &= \mu(1-x_1^2)x_2 - x_1 \end{aligned} \tag{109}$$

Since the period of oscillation T is unknown in this example, we must apply the algorithm for the autonomous case from Section III. This is done by fixing $x_1(0) = 0$ and by replacing x_1 by T. Now if we apply either the discretized Newton method, or the secant method, to find the periodic solution with $\mu = 0.01$, we find either method will converge to Q_1 : $\left(x_1(0), x_2(0), T\right) = (0, 1.9977, 6.2832)$ when $x_2^0(0) > 1.3$ and $T(0) = 6.28$, or Q_2 : $\left(x_0(0), x_2(0), T\right) = (0, 0, 2\pi)$ when $x_2^0(0) < 0.7$ and $T(0) = 6.28$. The periodic solution corresponding to Q_1 can be shown to be stable, while that corresponding to Q_2 can be shown to be unstable. Hence unless we choose the initial value $x_2^0(0) < 0.7$, we will not expect a second periodic solution since it can never be observed in practice. However, if we apply the solution curves corresponding to two convenient initial guesses, these two solutions can be systematically identified. For example, if we choose P_1 : $\left(x_2^0(0), T\right) = (0.7, 6.28)$, P_2 : $\left(x_2^0(0), T\right) = (2.2, 6.28)$, we would obtain the two solution curves shown in Fig. 11(c), where only a portion of the second curve is shown because it leaves the right boundary at point A and returns at point B. The points corresponding to periodic solutions are then located at the intersection of the solution curves with the verticial line $\rho = 1$; namely, at Q_1 and Q_2.

As a further illustration of the application of the globally convergent algorithm, let us derive the relationship between the period of oscillation T, as well as the frequency response curves for the van der Pol oscillator as a

function of the parameter μ. This natural parameter suggests that we work with the augmented system (84). The results are shown in Figs. 12(a) and (b), respectively. Observe that $T \approx 2\pi$ for small μ but tends monotonically to a very large value as μ increases. Again, observe that the curves shown in Figs 12(a) and (b) are exact. To the best knowledge of the authors, such curves have been published only for small values of μ in order to guarantee that the higher harmonic components are negligible. Even then, they are not exact because of the approximations involved in the harmonic balance method. It is interesting to observe that the fundamental component of the van der Pol oscillator remains almost constant for all values of μ, even though the higher harmonic components increase monotonically with μ. For example, the solution waveforms corresponding to $\mu = 3.0$ will have a period $T \approx 8.86$ (from Fig. 12(a)) and will contain the 1st, 3rd, 5th, 7th and 9th harmonics whose amplitudes can be read off from Fig. 12(b). The resulting periodic waveforms for $x_1(t)$ and $x_2(t)$ are shown in Fig. 11(d).

VI. CONCLUDING REMARKS

Both the theoretical analysis and the examples show that the modified secant method is more efficient compared to the discretized Newton method, the efficiency increases as the size of the system increases. This is not surprising since the bulk of time needed to implement the shooting method is spent in doing transient analysis. Since the modified secant method requires only one analysis per iteration after the first step, as compared to n+1 analysis per iteration in the discretized Newton method, it is clear that the larger the system, the less efficient the latter will be.

The globally convergent algorithm is developed primarily for systems where a suitable initial guess is not easy to find. It is particularly attractive for finding multiple periodic solutions, especially those frequently encountered in the area of nonlinear oscillation. In this case, no other algorithms (other than the brute force transient analysis method) of comparable accuracy presently exist. In fact, for strongly nonlinear systems with many harmonic components, our algorithm appears to be the only practical computation method available.

APPENDIX 1. Explicit Formula for Reduced System of Implicit Equations

Let N be a nonlinear network containing voltage or current-controlled 2-terminal resistors, voltage-controlled 2-terminal capacitors, current-controlled 2-terminal inductors, as well as independent and controlled sources. Mutual couplings are allowed so long as they are restricted to elements belonging to the same class. Let each independent source be considered as part of a "composite" branch as in [10]. Adopting the notations in Section 17-2 of [10], we obtain the following tableau equation for N:

$$\begin{bmatrix} \underset{\sim}{1} & -\underset{\sim}{A}^T & \underset{\sim}{0} \\ \underset{\sim}{K}_v & \underset{\sim}{0} & \underset{\sim}{K}_i \\ \underset{\sim}{0} & \underset{\sim}{0} & \underset{\sim}{A} \end{bmatrix} \begin{bmatrix} \underset{\sim}{v} \\ \underset{\sim}{v}_n \\ \underset{\sim}{i} \end{bmatrix} - \begin{bmatrix} \underset{\sim}{E} \\ \underset{\sim}{g}(\dot{\underset{\sim}{v}}_C, \dot{\underset{\sim}{i}}_L, \underset{\sim}{v}, \underset{\sim}{i}) \\ \underset{\sim}{A}\ \underset{\sim}{J} \end{bmatrix} = \begin{bmatrix} \underset{\sim}{0} \\ \underset{\sim}{0} \\ \underset{\sim}{0} \end{bmatrix} \tag{A-1}$$

where the second equation contains the constitutive relations of all elements of N. Equation (A-1) consists of a system of 2b+n-1 implicit equations of the form (1), where "b" denotes the number of composite branches and "n" denotes the number of nodes. Our goal in this section is to derive an equivalent system of implicit equations containing fewer number of equations and variables for an important subclass of networks. In particular, we assume that N contains no loops of capacitors and independent voltage sources, no cut sets of inductors and independent current sources and that all controlled sources are current sources depending on either resistor or capacitor voltages. Consequently, there always exists a normal tree $\mathcal{T}$ containing all capacitors and no inductors [10]. If we let $\underset{\sim}{i}_2$ and $\underset{\sim}{v}_2$ denote the current and voltage vectors of all inductors in N, and let $\underset{\sim}{i}_1$ and $\underset{\sim}{v}_1$ denote the current and voltage vectors of the remaining elements, then (A-1) can be recast as follows:

$$\left[\begin{array}{cc:cc:c} \underset{\sim}{1} & \underset{\sim}{0} & -\underset{\sim}{Y}_b & \underset{\sim}{0} & \underset{\sim}{0} \\ \underset{\sim}{0} & \underset{\sim}{0} & \underset{\sim}{0} & \underset{\sim}{1} & \underset{\sim}{0} \\ \hdashline \underset{\sim}{0} & \underset{\sim}{0} & \underset{\sim}{1} & \underset{\sim}{0} & -\underset{\sim}{A}_1^T \\ \underset{\sim}{0} & \underset{\sim}{0} & \underset{\sim}{0} & \underset{\sim}{1} & -\underset{\sim}{A}_2^T \\ \hdashline \underset{\sim}{A}_1 & \underset{\sim}{A}_2 & \underset{\sim}{0} & \underset{\sim}{0} & \underset{\sim}{0} \end{array}\right] \left[\begin{array}{c} \underset{\sim}{i}_1 \\ \underset{\sim}{i}_2 \\ \hdashline \underset{\sim}{v}_1 \\ \underset{\sim}{v}_2 \\ \hdashline \underset{\sim}{v}_n \end{array}\right] - \left[\begin{array}{c} \underset{\sim}{g}(\dot{\underset{\sim}{v}}_c, \underset{\sim}{v}) \\ \underset{\sim}{L}(\underset{\sim}{i}_2)\dot{\underset{\sim}{i}}_2 \\ \hdashline \underset{\sim}{E}_1 \\ \underset{\sim}{E}_2 \\ \hdashline \underset{\sim}{A}\underset{\sim}{J} \end{array}\right] = \left[\begin{array}{c} \underset{\sim}{0} \\ \underset{\sim}{0} \\ \hdashline \underset{\sim}{0} \\ \underset{\sim}{0} \\ \hdashline \underset{\sim}{0} \end{array}\right] \tag{A-2}$$

where the reduced incidence matrix is similarly partitioned into $\underset{\sim}{A} = [\underset{\sim}{A}_1\ \underset{\sim}{A}_2]$, and where $\underset{\sim}{L}(\underset{\sim}{i}_2)$ denotes the incremental inductance matrix. Substituting

$$\underset{\sim}{i}_1 = \underset{\sim}{Y}_b \underset{\sim}{v}_1 + \underset{\sim}{g}(\dot{\underset{\sim}{v}}_c, \underset{\sim}{v}) = \underset{\sim}{Y}_b(\underset{\sim}{A}_1^T \underset{\sim}{v}_n + \underset{\sim}{E}_1) + \underset{\sim}{g}(\dot{\underset{\sim}{v}}_c, \underset{\sim}{v}) \tag{A-3}$$

into the last equation in (A-2), we obtain the following reduced system of equations:

$$\underset{\sim}{A}_2\underset{\sim}{i}_2 + (\underset{\sim}{A}_1\underset{\sim}{Y}_b\underset{\sim}{A}_1^T)\underset{\sim}{v}_n = -\underset{\sim}{A}_1\underset{\sim}{Y}_b\underset{\sim}{E}_1 - \underset{\sim}{A}_1\underset{\sim}{g}(\dot{\underset{\sim}{v}}_c,\underset{\sim}{v}) + \underset{\sim}{A}\underset{\sim}{J} \tag{A-4}$$

$$\underset{\sim}{v}_2 = \underset{\sim}{A}_2^T\underset{\sim}{v}_n + \underset{\sim}{E}_2 = \underset{\sim}{L}(\underset{\sim}{i}_2)\dot{\underset{\sim}{i}}_2 \tag{A-5}$$

Let $\underset{\sim}{v}_{\mathcal{T}}$ denote the branch voltage vector associated with the normal tree $\mathcal{T}$, and let $\underset{\sim}{v}_{\mathcal{L}}$ denote the corresponding cotree voltages. Since all capacitors are assigned in $\mathcal{T}$, $\underset{\sim}{v}_C$ is a subvector of $\underset{\sim}{v}_{\mathcal{T}}$. Similarly, since all inductors are assigned in the cotree, $\underset{\sim}{v}_2$ is a subvector of $\underset{\sim}{v}_{\mathcal{L}}$. Let the reduced incidence matrix $\underset{\sim}{A}$ be partitioned accordingly into $\underset{\sim}{A}_{\mathcal{T}}$ and $\underset{\sim}{A}_{\mathcal{L}}$, so that KVL assumes the form

$$\underset{\sim}{v} \triangleq \begin{bmatrix}\underset{\sim}{v}_{\mathcal{T}}\\ \hdashline \underset{\sim}{v}_{\mathcal{L}}\end{bmatrix} = \begin{bmatrix}\underset{\sim}{A}_{\mathcal{T}}\\ \hdashline \underset{\sim}{A}_{\mathcal{L}}\end{bmatrix}^T \underset{\sim}{v}_n + \begin{bmatrix}\underset{\sim}{E}_{\mathcal{T}}\\ \underset{\sim}{E}_{\mathcal{L}}\end{bmatrix} \tag{A-6}$$

Since the columns of $\underset{\sim}{A}_{\mathcal{T}}$ correspond to tree branches, $\underset{\sim}{A}_{\mathcal{T}}$ is non-singular [10]. Hence we can solve for the node-to-datum voltage vector $\underset{\sim}{v}_n$ from (A-6) to obtain

$$\underset{\sim}{v}_n = [\underset{\sim}{A}_{\mathcal{T}}^T]^{-1}[\underset{\sim}{v}_{\mathcal{T}} - \underset{\sim}{E}_{\mathcal{T}}] \tag{A-7}$$

$$\underset{\sim}{v}_{\mathcal{L}} = \underset{\sim}{A}_{\mathcal{L}}^T[\underset{\sim}{A}_{\mathcal{T}}^T]^{-1}[\underset{\sim}{v}_{\mathcal{T}} - \underset{\sim}{E}_{\mathcal{T}}] + \underset{\sim}{E}_{\mathcal{L}} \tag{A-8}$$

Substituting (A-7) and (A-8) into (A-4) and (A-5), and denoting the inductor current vector $\underset{\sim}{i}_2$ by $\underset{\sim}{i}_L$, we obtain

$$\boxed{\underset{\sim}{A}_2\underset{\sim}{i}_L + \left(\underset{\sim}{A}_1\underset{\sim}{Y}_b\underset{\sim}{A}_1^T\right)\left[\underset{\sim}{A}_{\mathcal{T}}^T\right]^{-1}(\underset{\sim}{v}_{\mathcal{T}} - \underset{\sim}{E}_{\mathcal{T}}) = -\underset{\sim}{A}_1\underset{\sim}{Y}_b\underset{\sim}{E}_1 - \underset{\sim}{A}_1\hat{\underset{\sim}{g}}(\dot{\underset{\sim}{v}}_c,\underset{\sim}{v}_{\mathcal{T}}) + \underset{\sim}{A}\underset{\sim}{J}} \tag{A-9}$$

$$\boxed{\underset{\sim}{A}_2^T[\underset{\sim}{A}_{\mathcal{T}}^T]^{-1}(\underset{\sim}{v}_{\mathcal{T}} - \underset{\sim}{E}_{\mathcal{T}}) + \underset{\sim}{E}_2 = \underset{\sim}{L}(\underset{\sim}{i}_L)\dot{\underset{\sim}{i}}_L} \tag{A10}$$

where

$$\hat{\underset{\sim}{g}}(\dot{\underset{\sim}{v}}_c,\underset{\sim}{v}_{\mathcal{T}}) \triangleq \underset{\sim}{g}(\dot{\underset{\sim}{v}}_c,\underset{\sim}{v})\Big|_{\underset{\sim}{v} = [\underset{\sim}{v}_{\mathcal{T}}\underset{\sim}{v}_{\mathcal{L}}]^T} \tag{A-11}$$

and $\underset{\sim}{v}_{\mathcal{L}}$ is given by (A-8).

Equations (A-9)-(A-10) constitute a reduced system of implicit equations in terms of the state variables $\underset{\sim}{x} \triangleq [\underset{\sim}{v}_C\underset{\sim}{i}_L]^T$ and the non-state variables contained within $\underset{\sim}{v}_{\mathcal{T}}$.

Equation (A-9) can be interpreted as the nodal equation of N with all inductor currents i_{L_j} considered as independent sources, and with all node-to-datum voltages expressed in terms of the normal tree voltage vector $\underset{\sim}{v}_{\mathcal{T}}$. Similarly, (A-10) can be interpreted as the fundamental loop equations (relative to the normal tree $\mathcal{T}$) formed by the inductor links. These

interpretations allow us to write down the reduced system of implicit equations of simple nonlinear networks -- such as those considered in Section V -- by inspection. If N contains loops of capacitors and independent voltage sources, or cut sets of inductors and independent current sources, the above procedure can be easily generalized by first expressing the cotree capacitor voltages in terms of tree capacitor voltages, and tree inductor currents in terms of cotree inductor currents [10].

APPENDIX 2. Proof of the Secant Method Convergence Lemma

Applying the secant algorithm to (61), we obtain

$$\underset{\sim}{u}^{j+1}(0) = \underset{\sim}{u}^{j}(0) - (\underset{\sim}{H}^{j})(\underset{\sim}{\Gamma}^{j})^{-1}\hat{\underset{\sim}{F}}\left(\underset{\sim}{u}^{j}(0)\right) \tag{A-12}$$

If we let

$$\underset{\sim}{J}^{j} \triangleq (\underset{\sim}{\Gamma}^{j})(\underset{\sim}{H}^{j})^{-1} \tag{A-13}$$

then we can write

$$(\underset{\sim}{J}^{j})(\underset{\sim}{H}^{j}) = \underset{\sim}{\Gamma}^{j} \tag{A-14}$$

It follows from (A-14), (29) and (30) that

$$\hat{\underset{\sim}{F}}\left(\underset{\sim}{u}^{j-m}(0)\right) - \hat{\underset{\sim}{F}}\left(\underset{\sim}{u}^{j-m-1}(0)\right) = (\underset{\sim}{J}^{j})\left(\underset{\sim}{u}^{j-m}(0) - \underset{\sim}{u}^{j-m-1}(0)\right)$$

or,

$$\hat{\underset{\sim}{F}}\left(\underset{\sim}{u}^{j-m}(0)\right) - (\underset{\sim}{J}^{j})\underset{\sim}{u}^{j-m}(0) = \hat{\underset{\sim}{F}}\left(\underset{\sim}{u}^{j-m-1}(0)\right) - (\underset{\sim}{J}^{j})\underset{\sim}{u}^{j-m-1}(0),\ m = 0,1,2,\ldots,n-1$$

Hence

$$\begin{aligned}\underset{\sim}{C}^{j} &\triangleq \hat{\underset{\sim}{F}}\left(\underset{\sim}{u}^{j}(0)\right) - (\underset{\sim}{J}^{j})\underset{\sim}{u}^{j}(0) = \hat{\underset{\sim}{F}}\left(\underset{\sim}{u}^{j-1}(0)\right) - (\underset{\sim}{J}^{j})\underset{\sim}{u}^{j-1}(0) \\ &= \ldots\ldots = \hat{\underset{\sim}{F}}\left(\underset{\sim}{u}^{j-n+1}(0)\right) - (\underset{\sim}{J}^{j})\underset{\sim}{u}^{j-n+1}(0)\end{aligned} \tag{A-15}$$

Combining all vectors of (A-15), we obtain

$$\begin{bmatrix} \hat{F}_1\left(\underset{\sim}{u}^{j-n}(0)\right) & \hat{F}_1\left(\underset{\sim}{u}^{j-n+1}(0)\right) & \cdots & \hat{F}_1\left(\underset{\sim}{u}^{j}(0)\right) \\ \hat{F}_2\left(\underset{\sim}{u}^{j-n}(0)\right) & \hat{F}_2\left(\underset{\sim}{u}^{j-n+1}(0)\right) & \cdots & \hat{F}_2\left(\underset{\sim}{u}^{j}(0)\right) \\ \vdots & \vdots & \cdots & \vdots \\ \hat{F}_n\left(\underset{\sim}{u}^{j-n}(0)\right) & \hat{F}_n\left(\underset{\sim}{u}^{j-n+1}(0)\right) & \cdots & \hat{F}_n\left(\underset{\sim}{u}^{j}(0)\right) \end{bmatrix} - \begin{bmatrix} J_{11} & J_{12} & \cdots & J_{1n} \\ J_{21} & J_{22} & \cdots & J_{2n} \\ \vdots & \vdots & \cdots & \vdots \\ J_{n1} & J_{n2} & \cdots & J_{nn} \end{bmatrix} \begin{bmatrix} u_1^{j-n}(0) & u_1^{j-n+1}(0) & \cdots & u_1^{j}(0) \\ u_2^{j-n}(0) & u_2^{j-n+1}(0) & \cdots & u_2^{j}(0) \\ \vdots & \vdots & \cdots & \vdots \\ u_n^{j-n}(0) & u_n^{j-n+1}(0) & \cdots & u_n^{j}(0) \end{bmatrix} + \begin{bmatrix} C_1^j & C_1^j & \cdots & C_1^j \\ C_2^j & C_2^j & \cdots & C_2^j \\ \vdots & \vdots & \cdots & \vdots \\ C_n^j & C_n^j & \cdots & C_n^j \end{bmatrix}$$

(A-16)

where $\underset{\sim}{J}$ is defined by (A-13). Equation (A-16) can be written compactly as follows:

$$\hat{\underset{\sim}{F}}^j = (\underset{\sim}{J}^j)(\underset{\sim}{U}^j) + (\underset{\sim}{C}^j)(\underset{\sim}{I}) \tag{A-17}$$

where

$$\hat{\underset{\sim}{F}}^j \triangleq \left[\hat{\underset{\sim}{F}}\left(\underset{\sim}{u}^{j-n}(0)\right) \;\; \hat{\underset{\sim}{F}}\left(\underset{\sim}{u}^{j-n+1}(0)\right) \;\; . \;\; . \;\; . \;\; . \;\; . \;\; \hat{\underset{\sim}{F}}\left(\underset{\sim}{u}^{j}(0)\right)\right]$$

$$\underset{\sim}{U}^j \triangleq \left[\underset{\sim}{u}^{j-n}(0) \;\; \underset{\sim}{u}^{j-n+1}(0) \;\; . \;\; . \;\; . \;\; . \;\; . \;\; \underset{\sim}{u}^{j}(0)\right]$$

$$\underset{\sim}{I} \triangleq [1 \; 1 \; 1 \; . \; . \; . \; . \; . \; 1]$$

The $\underline{i}$th row of (A-17) can be written as follows:

$$\hat{\underset{\sim}{F}}_i^j = [\underset{\sim}{J}^j \;\; \underset{\sim}{C}^j]_i \begin{bmatrix} \underset{\sim}{U}^j \\ \underset{\sim}{I} \end{bmatrix} \tag{A-18}$$

Transposing both sides of (A-18), we obtain

$$[(\underset{\sim}{U}^j)^T \vdots \underset{\sim}{I}^T] \begin{bmatrix} (\underset{\sim}{J}^j)_i^T \\ \hline C_i^j \end{bmatrix} = (\underset{\sim}{F}_i^j)^T \tag{A-19}$$

When expanded, (A-19) can be recast into the following system of linear equations:

$$\left[\begin{array}{cccc:c} u_1^{j-n}(0) & u_2^{j-n}(0) & . \; . \; . \; . & u_n^{j-n}(0) & 1 \\ u_1^{j-n+1}(0) & u_2^{j-n+1}(0) & . \; . \; . \; . & u_n^{j-n+1}(0) & 1 \\ . & . & . \; . \; . \; . & . & . \\ . & . & . \; . \; . \; . & . & . \\ u_1^{j}(0) & u_2^{j}(0) & . \; . \; . \; . & u_n^{j}(0) & 1 \end{array}\right] \left[\begin{array}{c} J_{i1}^j \\ J_{i2}^j \\ . \\ . \\ C_i^j \end{array}\right] = \left[\begin{array}{c} \hat{F}_i\left(\underset{\sim}{u}^{j-n}(0)\right) \\ \hat{F}_i\left(\underset{\sim}{u}^{j-n+1}(0)\right) \\ . \\ . \\ \hat{F}_i\left(\underset{\sim}{u}^{j}(0)\right) \end{array}\right] \tag{A-20}$$

Thus C_i^j can be solved using Cramer's formula:

$$C_i^j = \frac{\begin{vmatrix} u_1^{j-n}(0) & u_2^{j-n}(0) & \cdots & u_n^{j-n}(0) & \hat{F}_i\left(\underset{\sim}{u}^{j-n}(0)\right) \\ u_1^{j-n+1}(0) & u_2^{j-n+1}(0) & \cdots & u_n^{j-n+1}(0) & \hat{F}_i\left(\underset{\sim}{u}^{j-n+1}(0)\right) \\ \vdots & \vdots & \cdots & \vdots & \vdots \\ u_1^{j}(0) & u_2^{j} & \cdots & u_n^{j}(0) & \hat{F}_i\left(\underset{\sim}{u}^{j}(0)\right) \end{vmatrix}}{\begin{vmatrix} u_1^{j-n}(0) & u_2^{j-n}(0) & \cdots & u_n^{j-n}(0) & 1 \\ u_1^{j-n+1}(0) & u_2^{j-n+1}(0) & \cdots & u_n^{j-n+1}(0) & 1 \\ \vdots & \vdots & \cdots & \vdots & \vdots \\ u_1^{j}(0) & u_2^{j}(0) & \cdots & u_n^{j}(0) & 1 \end{vmatrix}} \qquad \text{(A-21)}$$

Now assume that the successive iterations give much closer approximations to the exact solution $\hat{\underset{\sim}{u}}(0) = \underset{\sim}{0}$. Thus

$$\|\underset{\sim}{u}^j(0)\| << \|\underset{\sim}{u}^{j-1}(0)\| << \cdots << \|\underset{\sim}{u}^{j-n}(0)\| \qquad \text{(A-22)}$$

The approximate value of the denominator of (A-21) can be estimated by expanding the determinant via the last row; i.e.

$$[\text{denominator of (A-21)}] = O\left\{\|\underset{\sim}{u}^{j-n}(0)\| \cdot \|\underset{\sim}{u}^{j-n+1}(0)\| \cdots \|\underset{\sim}{u}^{j-1}(0)\|\right\} \qquad \text{(A-23)}$$

where $O\{\cdot\}$ denotes that the [denominator of (A-21)] is of the order of the products of $\|\underset{\sim}{u}^{j-n}(0)\|, \ldots, \|\underset{\sim}{u}^{j-1}(0)\|$.

Substituting (A-12) into (A-21), the numerator of (A-21) can be estimated as follows:

$$[\text{numerator of (A-21)}] = O\left\{\sum_{k=1}^{n}\sum_{m=1}^{n} B_{i,km}|u_k^{j-n}(0)|\cdot|u_m^{j-n}(0)|\right\} \times O\left\{\|\underset{\sim}{u}^{j-n+1}(0)\| \cdot \|\underset{\sim}{u}^{j-n+2}(0)\| \cdots \|\underset{\sim}{u}^{j}(0)\|\right\} \qquad \text{(A-24)}$$

Hence there exists a constant B_i such that

$$[\text{numerator of (A-21)}] = B_i O\left\{\|\underset{\sim}{u}^{j-n}(0)\|^2\right\} \cdot O\left\{\|\underset{\sim}{u}^{j-n+1}(0)\| \|\underset{\sim}{u}^{j-n+2}(0)\| \cdots \|\underset{\sim}{u}^{j}(0)\|\right\} \qquad \text{(A-25)}$$

It follows from (A-23) and (A-25), that

$$C_i^j = \frac{\text{[numerator of (A-21)]}}{\text{[denominator of (A-21)]}}$$

$$= B_i \bigcirc \left\{ \frac{\|\underset{\sim}{u}^{j-n}(0)\|^2 \cdot \|\underset{\sim}{u}^{j-n+1}(0)\| \cdots \|\underset{\sim}{u}^{j-1}(0)\| \cdot \|\underset{\sim}{u}^{j}(0)\|}{\|\underset{\sim}{u}^{j-n}(0)\| \cdot \|\underset{\sim}{u}^{j-n+1}(0)\| \cdots \|\underset{\sim}{u}^{j-1}(0)\|} \right\}$$

$$= B_i \bigcirc \cdot \left\{ \|\underset{\sim}{u}^{j-n}\| \cdot \|\underset{\sim}{u}^{j}\| \right\} \qquad \text{(A-26)}$$

On the other hand, the secant algorithm (A-12) can be rewritten with the help of (A-13) and (A-15) into the following form:

$$\begin{aligned} \underset{\sim}{u}^{j+1}(0) &= \underset{\sim}{u}^{j}(0) - (\underset{\sim}{J}^{j})^{-1} \underset{\sim}{F}\left(u^{j}(0)\right) \\ &= (\underset{\sim}{J}^{j})^{-1} \left[(\underset{\sim}{J}^{j}) \underset{\sim}{u}^{j}(0) - \hat{\underset{\sim}{F}}\left(\underset{\sim}{u}^{j}(0)\right) \right] \\ &= -(\underset{\sim}{J}^{j})^{-1} \underset{\sim}{C}^{j} \end{aligned} \qquad \text{(A-27)}$$

Now since $\underset{\sim}{J}^{j}$ in (A-13) is nearly equal to the Jacobian matrix in the vicinity of $\hat{\underset{\sim}{u}}(0) = \underset{\sim}{0}$, $J^j \approx \underset{\sim}{1}$. It follows from (A-26) and (A-27) that

$$\begin{aligned} \|u^{j+1}(0)\| &\approx \|\underset{\sim}{C}^{j}\| \\ &= \|\underset{\sim}{B}^{j}\| \cdot \bigcirc \left\{ \|\underset{\sim}{u}^{j-n}(0)\| \cdot \|\underset{\sim}{u}^{j}(0)\| \right\}, \text{ for all } j \end{aligned} \qquad \text{(A-28)}$$

where $\underset{\sim}{B}^{j} \triangleq [B_1 \; B_2 \; \cdots \; B_n]^T$. Hence (A-28) implies

$$\|\underset{\sim}{u}^{j+1}(0)\| = B_s \|\underset{\sim}{u}^{j-n}(0)\| \cdot \|\underset{\sim}{u}^{j}(0)\| \qquad \text{(A-29)}$$

which is (62). ¤

REFERENCES

[1] Aprille, T.J., Jr. and Trick, T.N., "Steady-State analysis of nonlinear circuits with periodic input," Proc. IEEE, Vol. 60, Jan. 1972, pp. 108-114.

[2] Aprille, T.J., Jr. and Trick, T.N., A computer algorithm to determine the steady-state response of nonlinear oscillators," IEEE Trans. Circuit Theory, Vol. CT-19, July 1972, pp. 354-360.

[3] Trick, T.N., Colon, F.R., and Fan, S.P., "Computation of capacitor voltage and inductor current sensitivities with respect to initial conditions for the steady-state analysis of nonlinear periodic circuits," IEEE Trans. on Circuits and Systems, Vol. CAS-22, May 1975, pp. 391-396.

[4] Director, S.W., Broderson, A.J., and Wayne, D.A., "A method for quick determination of the periodic steady-state in nonlinear networks," Proc. 9th Annual Allerton Conference on Circuit and System Theory, University of Illinois, 131-319, 1971.

[5] Nakla, M.S. and Branin, F.H., Jr., "Determining the periodic response of nonlinear system by gradient method," International Journal of Circuit Theory and Applications, Vol. 5, July 1977, pp. 255-273.

[6] Hayashi, C., Nonlinear Oscillation in Physical Systems, McGraw-Hill, New York, N.Y., 1964.

[7] Urabe, M., "Galerkin's procedure for nonlinear periodic system," Arch. Rational Mech., Anal. 20, 1965, pp. 120-152.

[8] Nakhla, M.S. and Vlach, J., "A piecewise harmonic balance technique for determination of periodic response of nonlinear systems," IEEE Trans. on Circuits and Systems, Vol. CAS-23, Feb. 1976, pp. 85-91.

[9] Gopal, K., Nakhla, M.S., Singhal, K., and Vlach, J., "Distortion analysis of transistor networks," IEEE Trans. on Circuits and Systems, Vol. CAS-25, February 1978, pp. 99-106.

[10] Chua, L.O. and Lin, P.M., Computer-Aided Analysis of Electronic Circuits: Algorithms and Computational Techniques, Prentice-Hall, Englewood Cliffs, N.J., 1975.

[11] Chua, L.O. and Sing, Y.W., "A nonlinear dumped circuit model for Gunn diodes," International Journal of Circuit Theory and Applications, in press.

[12] Chua, L.O. and Ushida, A., "A switching parameter algorithm for finding multiple solutions of nonlinear resistive circuits," International Journal of Circuit Theory and Applications, Vol. 4, 1976, pp. 215-239.

[13] Hale, J.K., Ordinary Differential Equations, Wiley-Interscience, New York, 1969.

[14] Ortega, J.M. and Rheinboldt, W.C., Iterative solution of nonlinear equations in several variables, Academic Press, New York, N.Y. 1970.

[15] Barnes, J., "An algorithm for solving nonlinear equations based on the secant method," Comput. J., Vol. 8, 1965, pp. 66-72.

[16] Ueda, Y., Some Problems in the Thoery of Nonlinear Oscillations, Nippon Printing and Publishing Co. LTD., Osaka Japan, 1968.

LIST OF FIGURE CAPTIONS

Fig. 1. Geometrical interpretation of the one-dimensional secant method.

Fig. 2. The unknown period T for an autonomous circuit is obtained by first choosing a time origin such that $|x_p(0)| < C$ and by equating $x_p(T) = x_p(0)$.

Fig. 3. Geometrical interpretation of thw switching parameter algorithm in $\mathbb{R}^2$.

Fig. 4. (a) A high-Q bandpass filter. The circuit parameters are: R_1=1Ω, R_2=27kΩ, R_3=100Ω, R_4=100kΩ, R_5=1kΩ, R_6=27kΩ, R_7=100Ω, R_8=100kΩ, R_9=1kΩ, R_{10}=10KΩ, C_1 = 0.1μF, C_2=20μF, C_3=100μF, C_4=0.1μF, C_5=100μF C_6=2μF, C_7=2μF, L_8=10H, L_9=0.05H, L_{10}=10H, E_b=+15(V), $v_{in}=E_m \sin \omega T$.

(b) The dc Ebers-Moll transistor circuit model $I_{di1} = 10^{-8}[e^{40v_{EB}}-1]$, $I_{di2} = 10^{-8}[e^{40v_{EC}}-1]$, and $\alpha = 0.99$.

Fig. 5. Number of transient analyses of the bandpass filter over [0,T] using 4 different methods: 1) brute force transient analysis, 2) discretized Newton method, 3) secant method, and 4) modified secant method.

Fig. 6. Periodic output voltage solution $v_{out}(t)$.
(a) ω = 990 rad./sec. (b) ω = 1040 rad./sec.

Fig. 7. (a) A modified Colpitt sine-cosine oscillator. The circuit parameters are: R_1=17KΩ, R_2=10KΩ, R_3=390Ω, R_4=910Ω, R_5=10KΩ, $430\Omega \leq R_6 \leq 460\Omega$, R_7=150Ω, R_8=47KΩ, R_9=22KΩ, R_{10}=470Ω, C_1=0.1μF, C_2=0.1μF, C_3=0.5μF, L_4=0.3H, L_5=0.5H, and E_b=-12 volts. The transistors are modeled by Ebers-Moll model with $I_{i1}=10^{-7}[e^{40v_{EB}}-1]$, $I_{i2}=10^{-7}[e^{40v_{CB}}-1]$, i=1,2,3, α=0.98.

(b) Output voltage waveforms with R = 450Ω.

(c) Output voltage waveforms with R = 430Ω.

Fig. 8. (a) The region of absolute stability for 4th order BDF:

(b) Convergence behavior of modified secant method for 3 different parameter values of R_6.

Fig. 9. (a) A nonlinear RLC resonant circuit described by Duffing's equation.

(b) Solution curves corresponding to 4 different initial points P_1, P_2, P_3 and P_4. The three intersections Q_1, Q_2, and Q_3 give the 3 T-periodic solutions.

(c) Nonlinear frequency response characteristic curves as a function of the input amplitude B.

Fig. 10. Nonlinear frequency response characteristic curves for 1/3 order subharmonics as a function of B.

(a) $0.10 \leq B \leq 0.25$

(b) $1.3 \leq B \leq 1.7$

(c) A 1/3 order subharmonic response $x_1(t)$ and $x_2(t)$ corresponding to $B = 0.1581$.

Fig. 11. (a) van der Pol oscillator circuit

(b) i_D-v_D curve of tunnel diode

(c) Determination of two periodic solutions using the globally convergent algorithm

(d) The periodic waveforms corresponding to $\mu = 3.0$ and $T = 8.8598$.

Fig. 12. (a) The oscillation period T -vs.- μ relationship for the van der Pol oscillator

(b) The freuqency response characteristics (amplitude of each harmonic component as a function of μ) for the van der Pol oscillator.

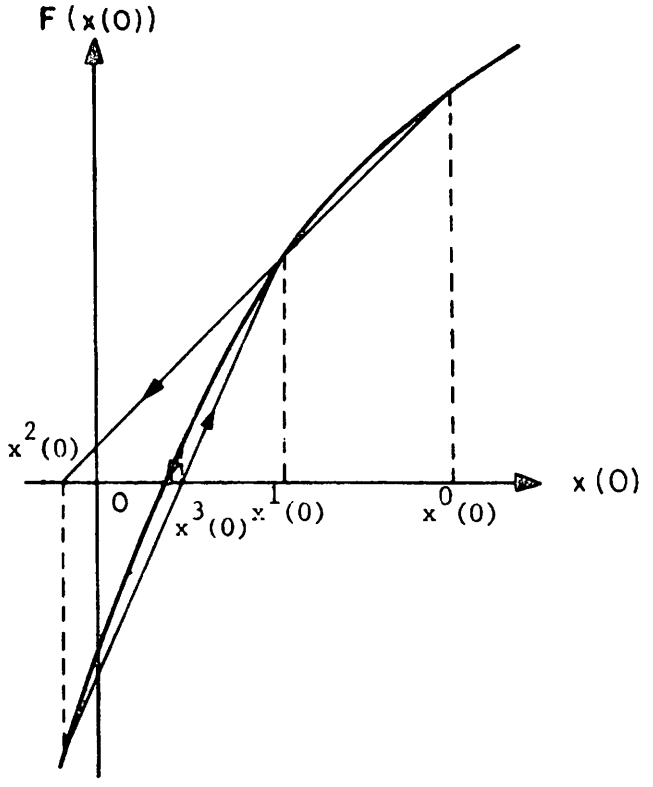

Fig. 1

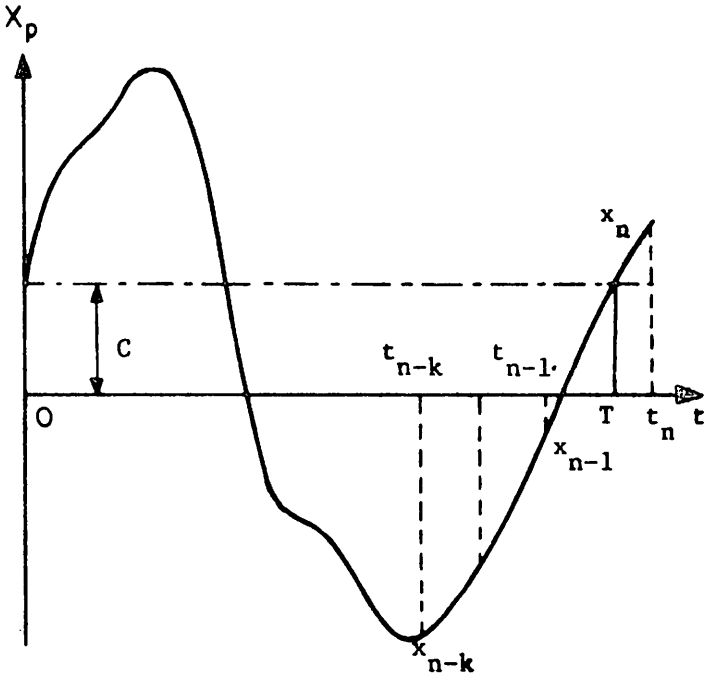

Fig. 2

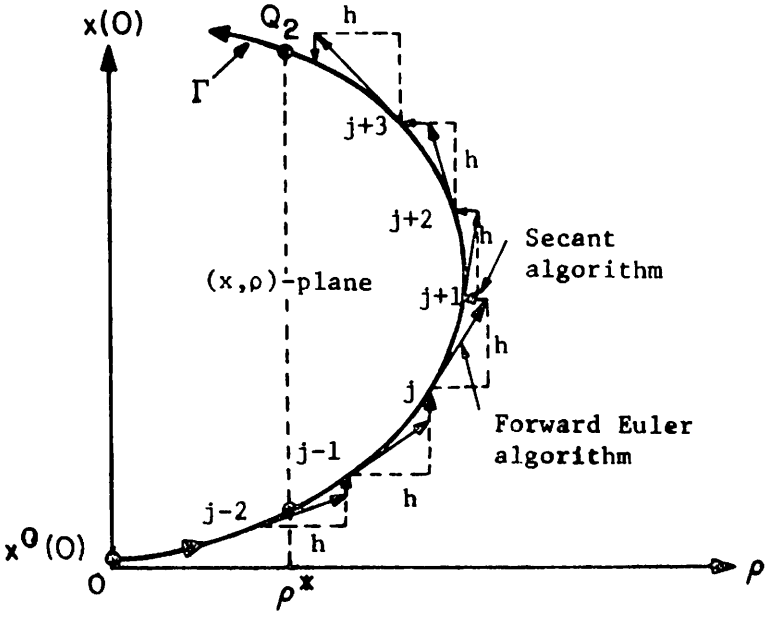

Fig. 3

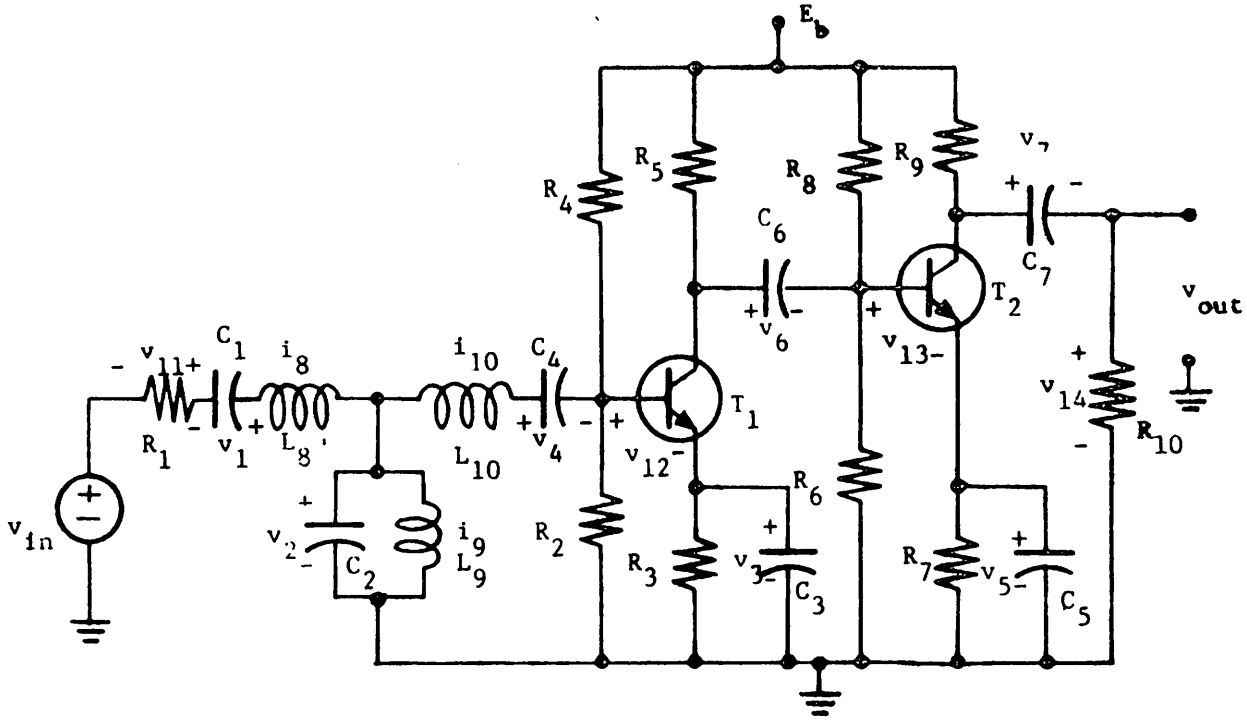
E_b
R_4
R_5
R_8
R_9
v_7
C_6
C_7
T_2
v_out
v_6
v_13
v_14
R_10
v_11
C_1
i_8
i_10
C_4
T_1
R_1
v_1
L_8
L_10
v_4
v_12
v_in
v_2
C_2
i_9
L_9
R_2
R_3
R_6
v_3
C_3
R_7
v_5
C_5

(a)

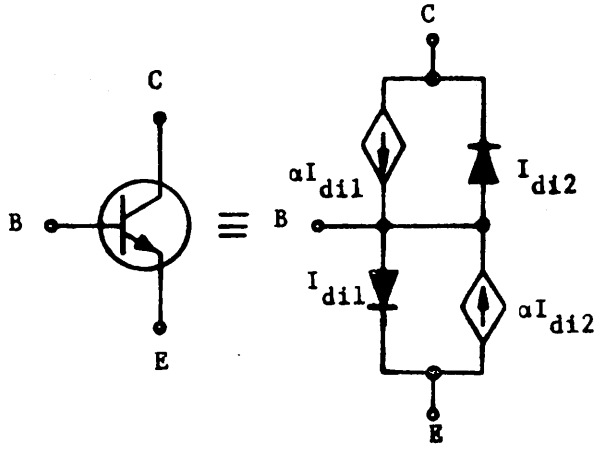
C
B
E
≡
αI_di1
I_di2
I_di1
αI_di2

(b)

Fig. 4

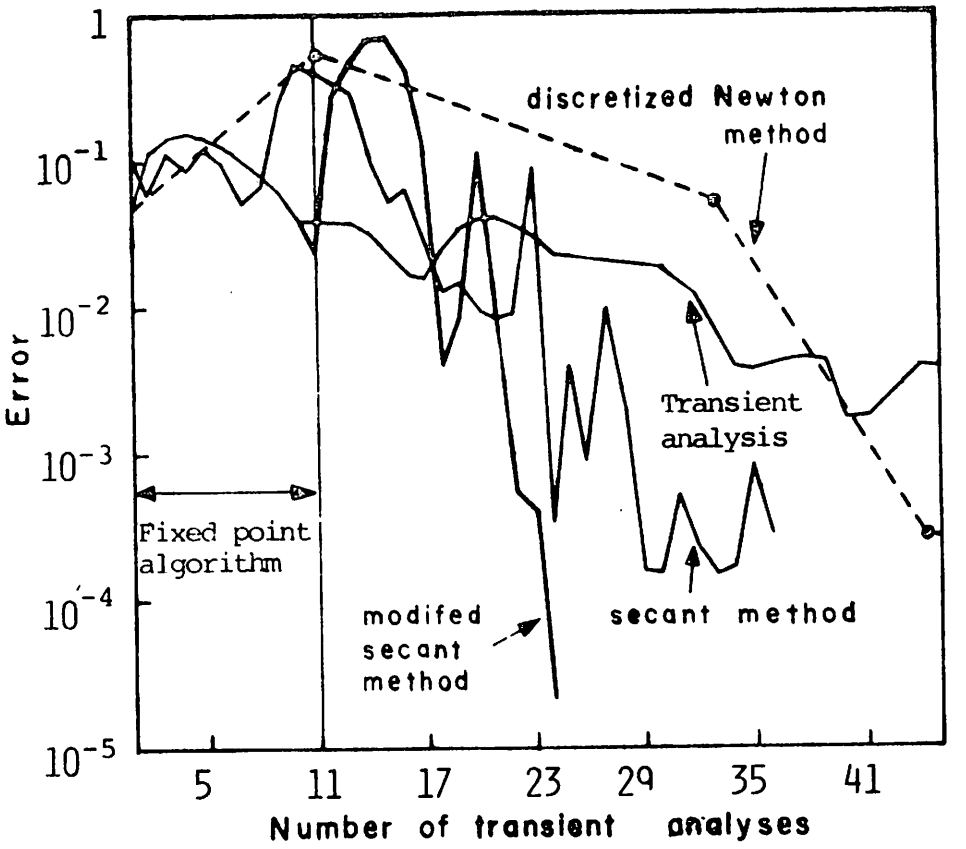
1
10^{-1}
10^{-2}
10^{-3}
10^{-4}
10^{-5}
Error
discretized Newton method
Transient analysis
Fixed point algorithm
modifed secant method
secant method
5
11
17
23
29
35
41
Number of transient analyses

Fig. 5

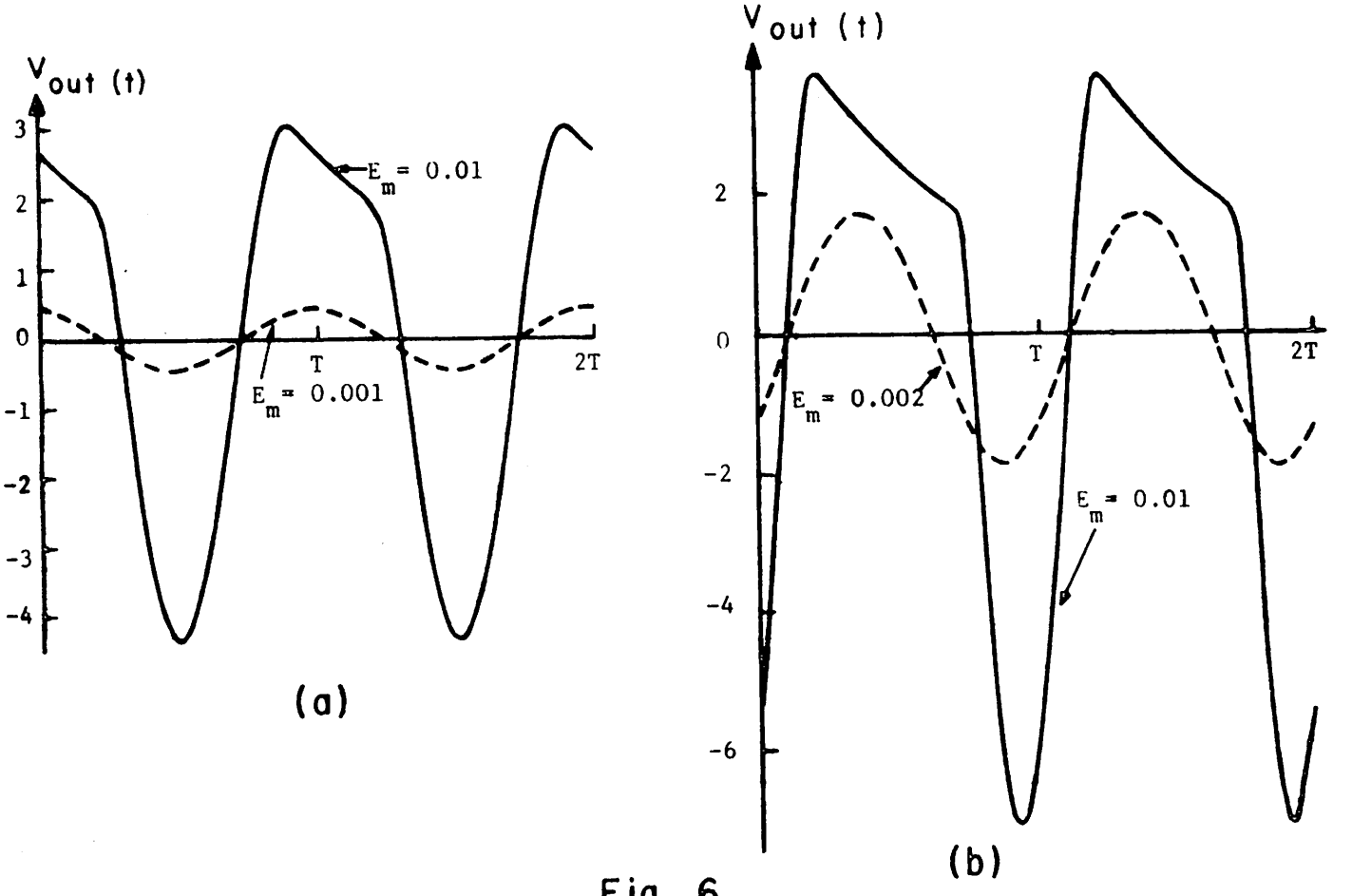
V_{out} (t)
3
2
1
0
-1
-2
-3
-4
E_m = 0.01
E_m = 0.001
T
2T
(a)
V_{out} (t)
2
0
-2
-4
-6
E_m = 0.002
E_m = 0.01
T
2T
(b)

Fig. 6

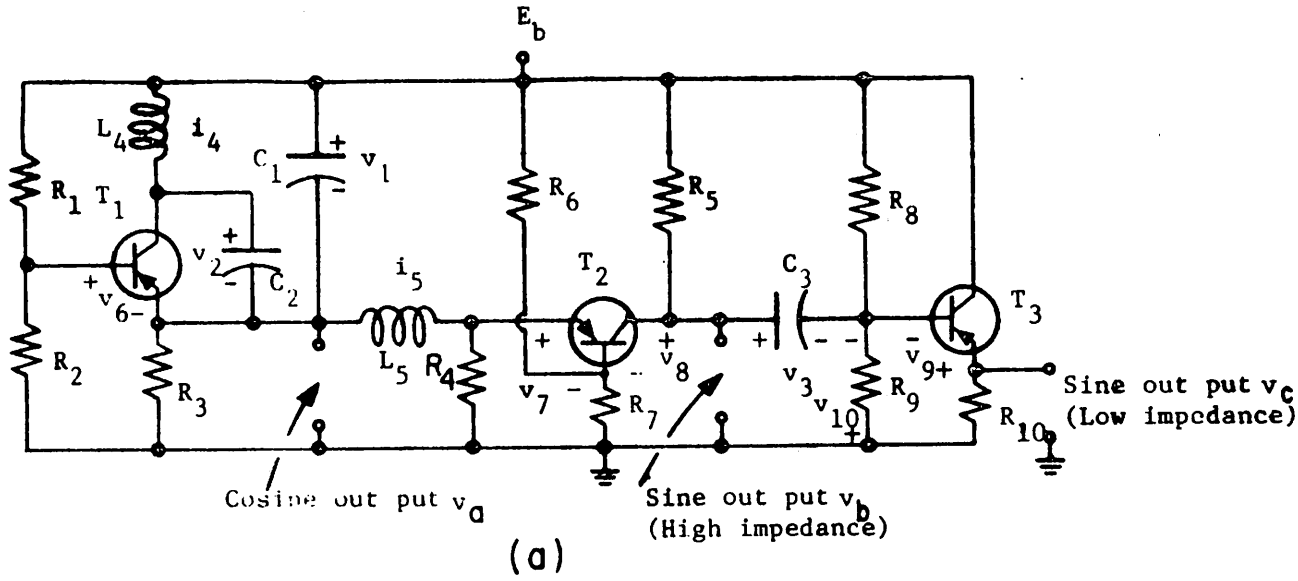
E_b
L_4
i_4
C_1
v_1
R_1
T_1
R_6
R_5
R_8
v_2
C_2
i_5
T_2
C_3
T_3
v_6
R_2
R_3
L_5
R_4
v_7
v_8
R_7
v_3
v_10
R_9
v_9
R_10
Sine out put v_c
(Low impedance)
Cosine out put v_a
Sine out put v_b
(High impedance)

(a)

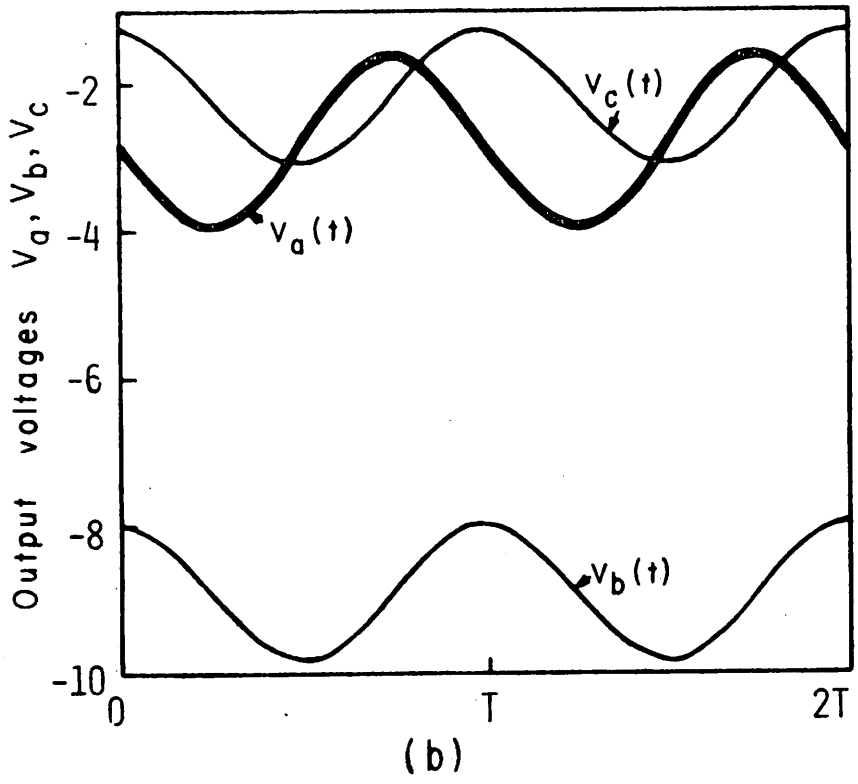
Output voltages V_a, V_b, V_c
-2
-4
-6
-8
-10
0
T
2T
V_c(t)
V_a(t)
V_b(t)

(b)

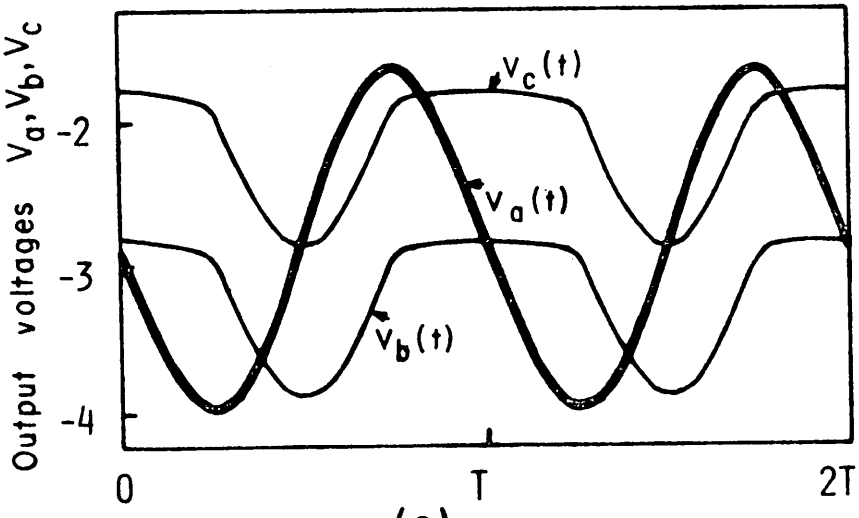
Output voltages V_a, V_b, V_c
-2
-3
-4
0
T
2T
V_c(t)
V_a(t)
V_b(t)

(c)

Fig. 7

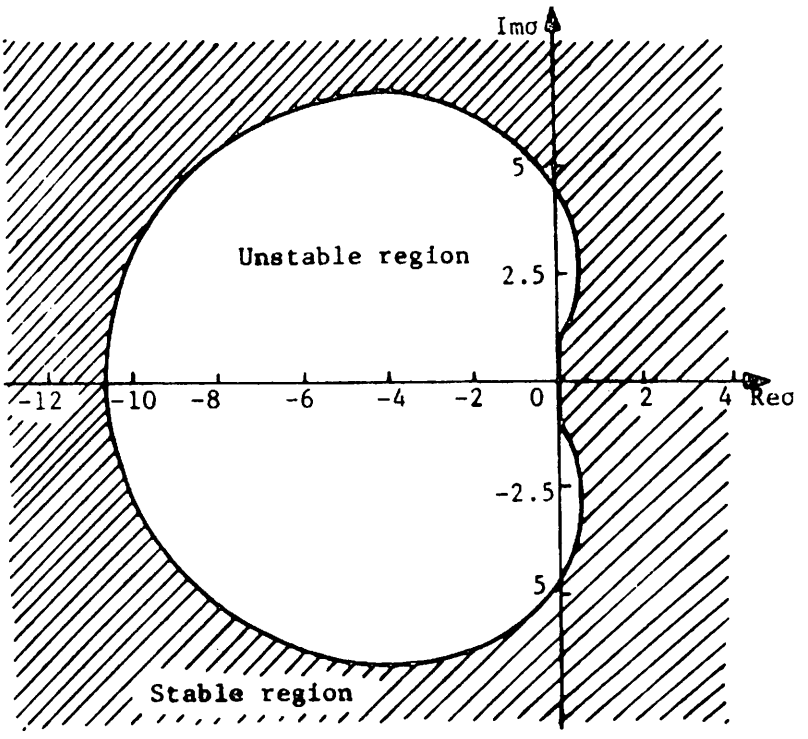
Imσ
5
Unstable region
2.5
-12
-10
-8
-6
-4
-2
0
2
4
Reσ
-2.5
5
Stable region

(a)

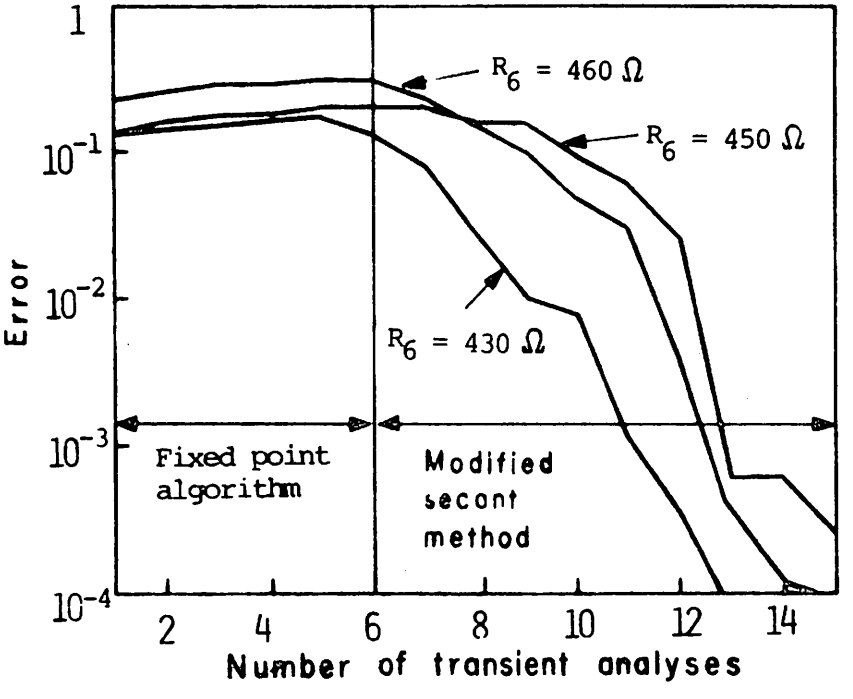
1
10^{-1}
10^{-2}
10^{-3}
10^{-4}
Error
R_6 = 460 Ω
R_6 = 450 Ω
R_6 = 430 Ω
Fixed point algorithm
Modified secont method
2
4
6
8
10
12
14
Number of transient analyses

(b)

Fig. 8

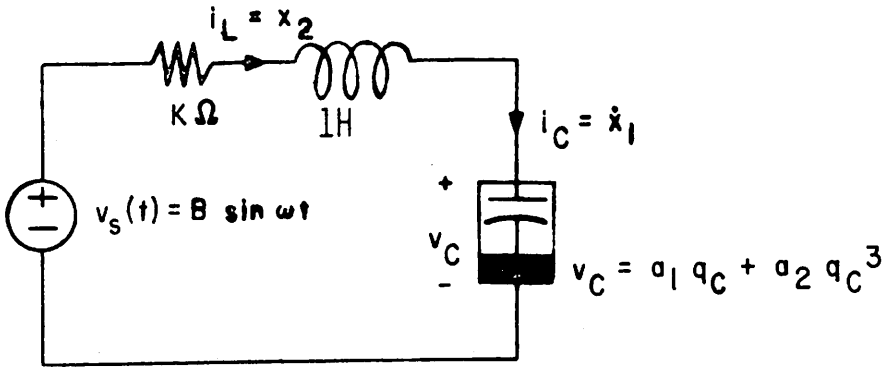
$i_L = x_2$
K Ω
1H
$i_C = \dot{x}_1$
$v_s(t) = B \sin \omega t$
v_C
$v_C = a_1 q_C + a_2 q_C^3$

(a)

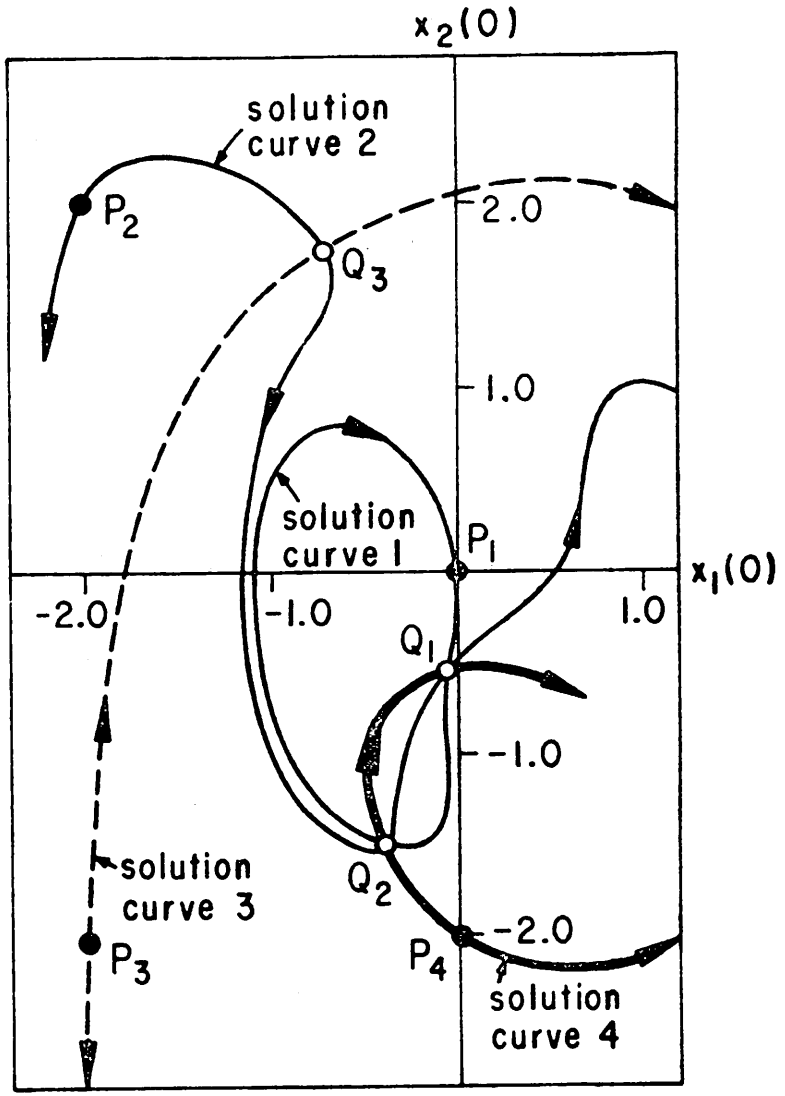
$x_2(0)$
solution curve 2
P_2
Q_3
2.0
1.0
solution curve 1
P_1
$x_1(0)$
-2.0
-1.0
1.0
Q_1
-1.0
solution curve 3
Q_2
P_3
P_4
-2.0
solution curve 4

(b)

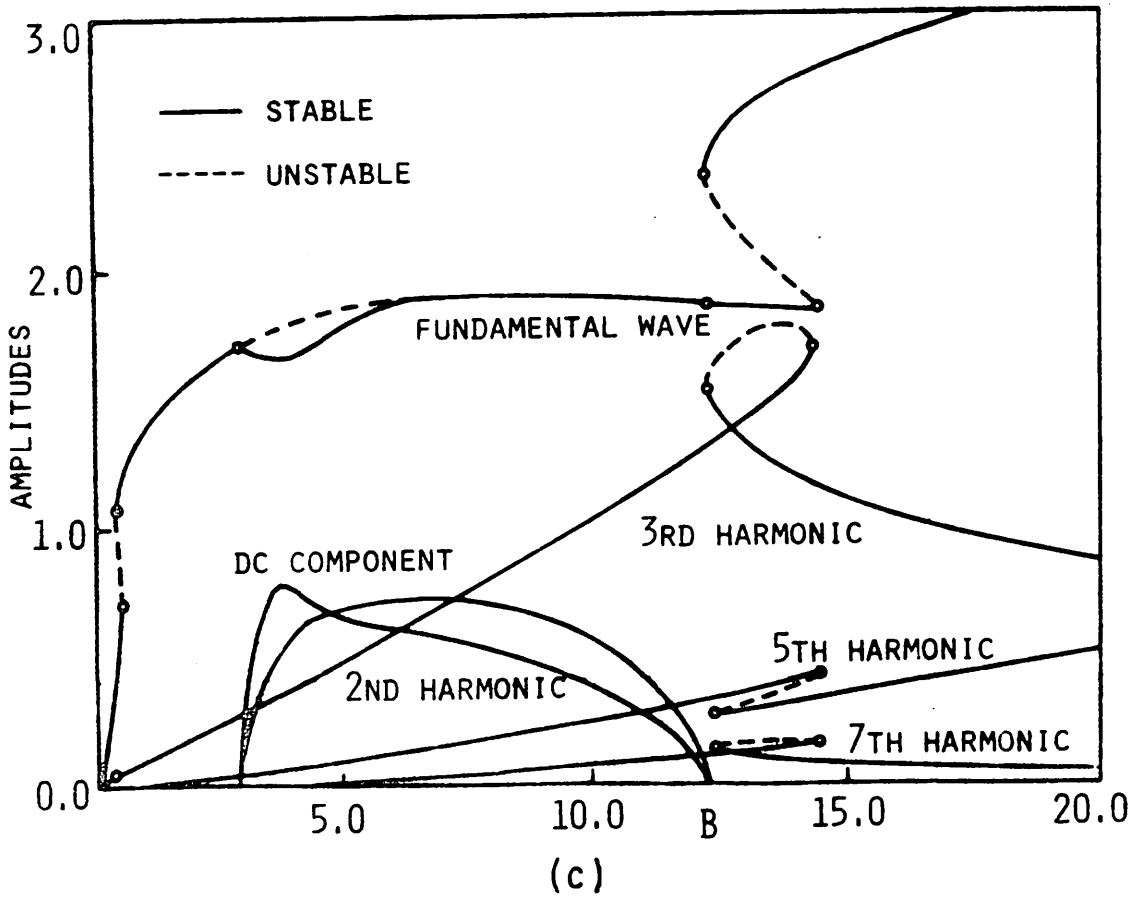
3.0
2.0
1.0
0.0
AMPLITUDES
STABLE
UNSTABLE
FUNDAMENTAL WAVE
3RD HARMONIC
DC COMPONENT
5TH HARMONIC
2ND HARMONIC
7TH HARMONIC
5.0
10.0
B
15.0
20.0

(c)

Fig. 9

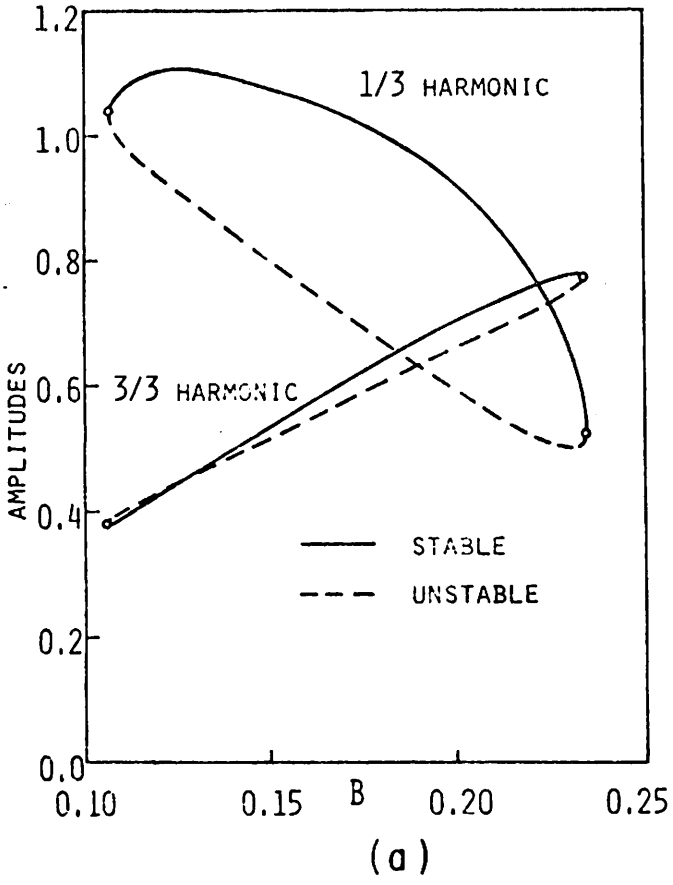
1.2
1.0
0.8
0.6
0.4
0.2
0.0
AMPLITUDES
1/3 HARMONIC
3/3 HARMONIC
STABLE
UNSTABLE
0.10
0.15
B
0.20
0.25

(a)

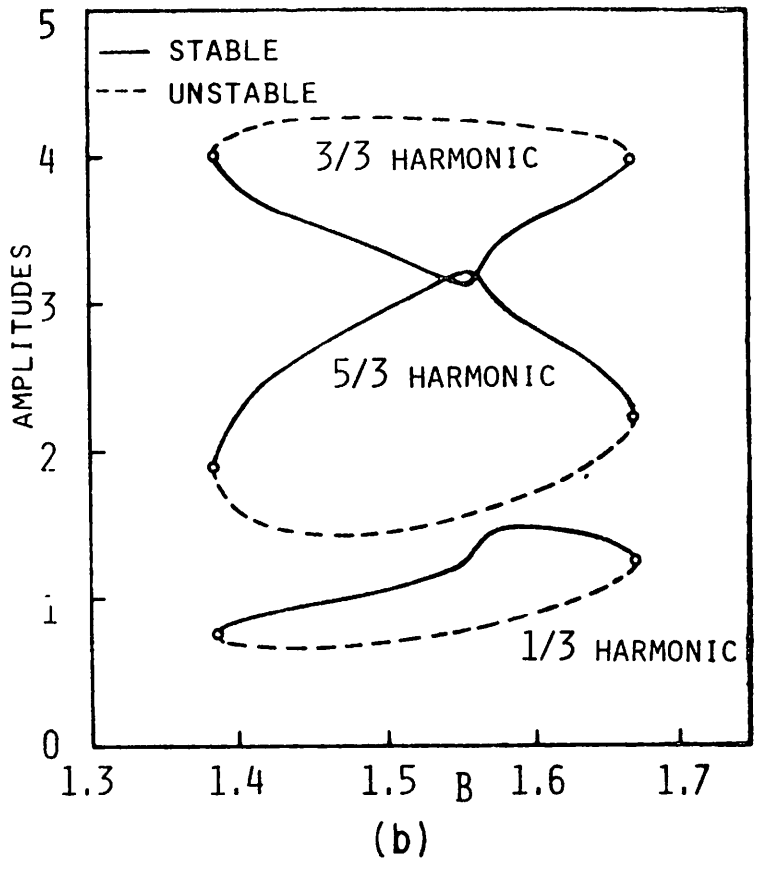
5
4
3
2
1
0
AMPLITUDES
STABLE
UNSTABLE
3/3 HARMONIC
5/3 HARMONIC
1/3 HARMONIC
1.3
1.4
1.5
B
1.6
1.7

(b)

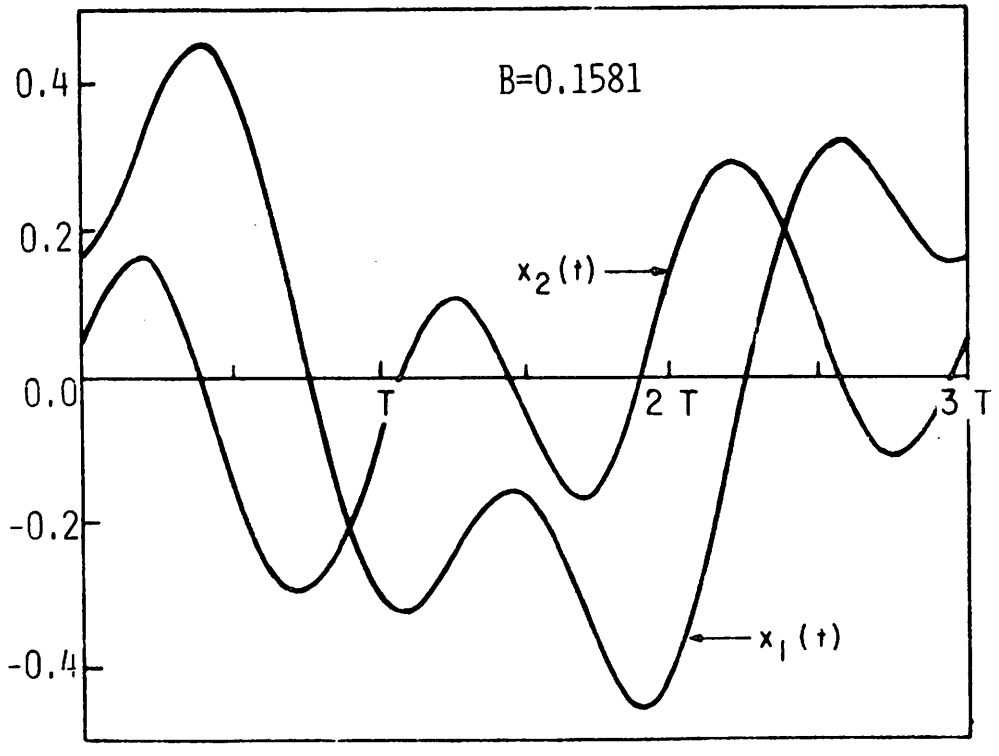
B=0.1581
0.4
0.2
0.0
-0.2
-0.4
$x_2(t)$
$x_1(t)$
T
2 T
3 T

(c)

Fig. 10

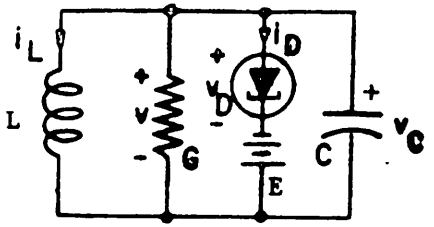
i_L
L
v
G
i_D
v_D
E
C
v_C

(a)

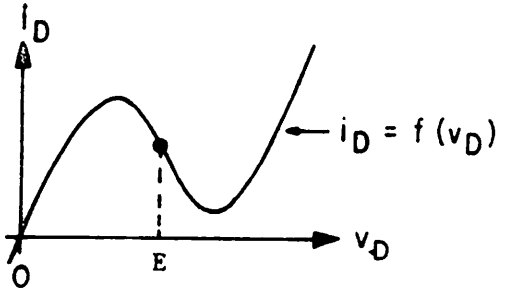
i_D
$i_D = f(v_D)$
v_D
O
E

(b)

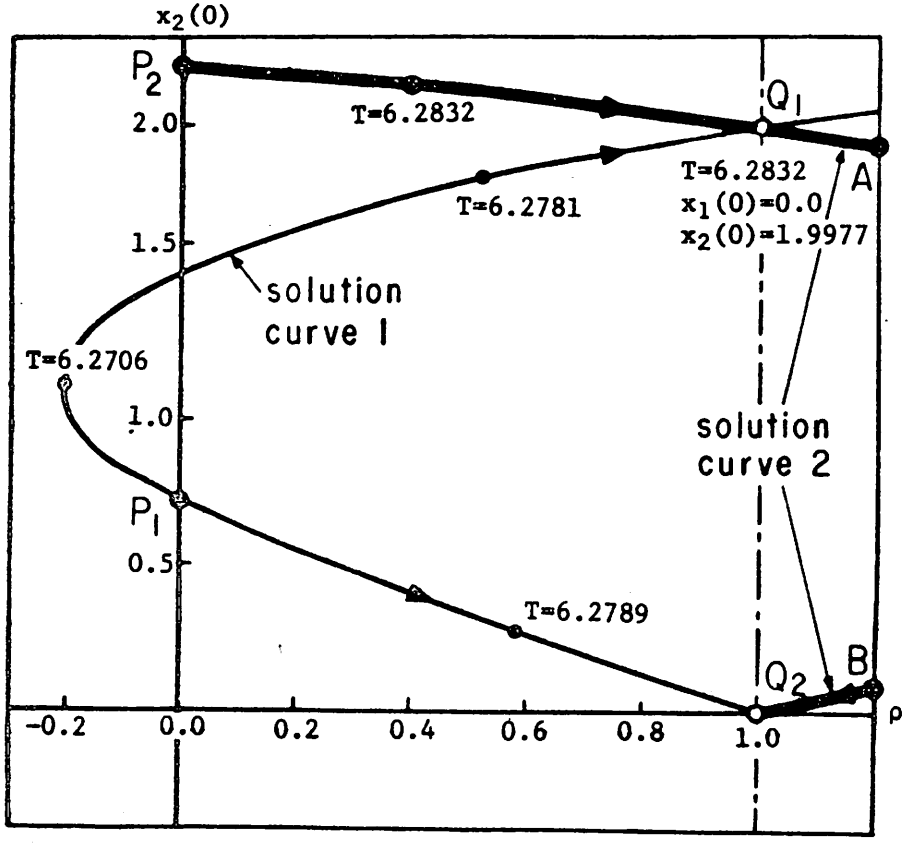
$x_2(0)$
P_2
2.0
1.5
1.0
P_1
0.5
T=6.2832
Q_1
T=6.2832
$x_1(0)=0.0$
$x_2(0)=1.9977$
A
T=6.2781
solution curve 1
T=6.2706
solution curve 2
T=6.2789
Q_2
B
-0.2
0.0
0.2
0.4
0.6
0.8
1.0
ρ

(c)

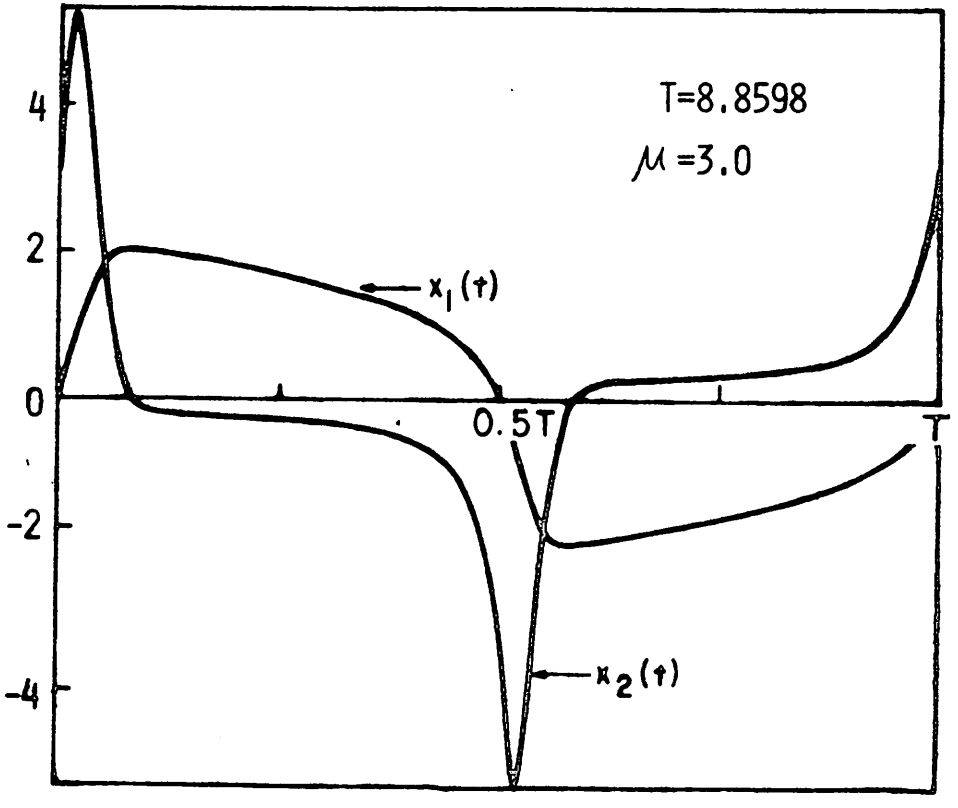
T=8.8598
$\mu=3.0$
4
2
0
-2
-4
$x_1(t)$
0.5T
T
$x_2(t)$

(d)

Fig. 11

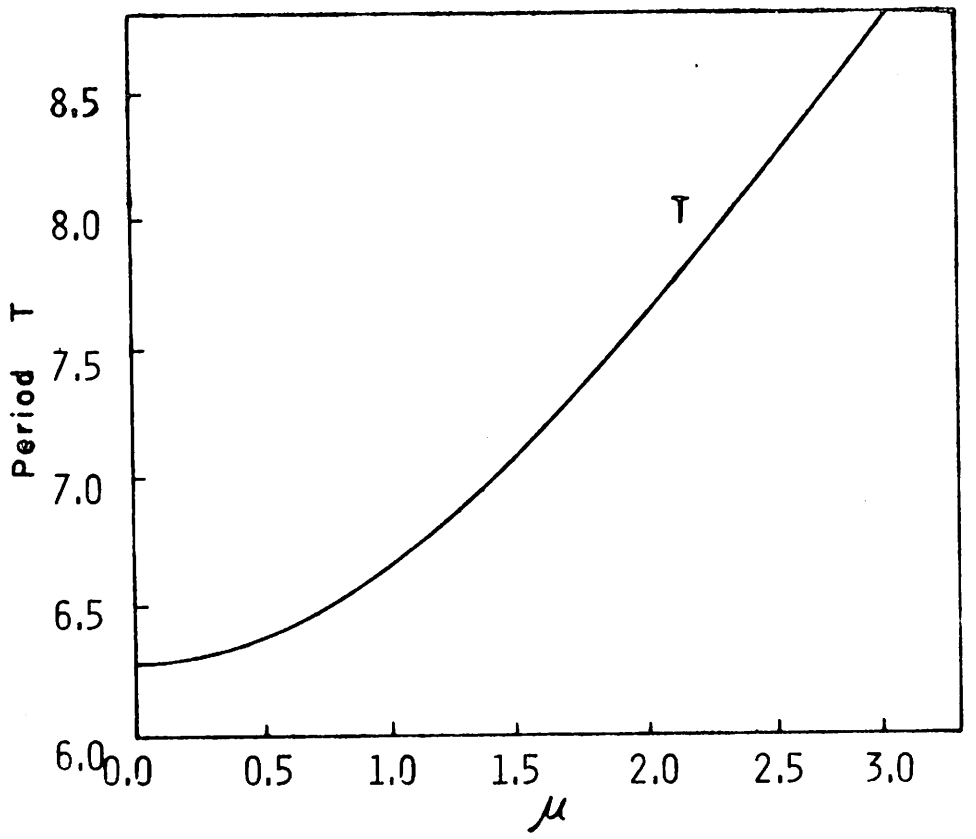
8.5
8.0
7.5
7.0
6.5
6.0
Period T
T
0.0
0.5
1.0
1.5
2.0
2.5
3.0
μ

(a)

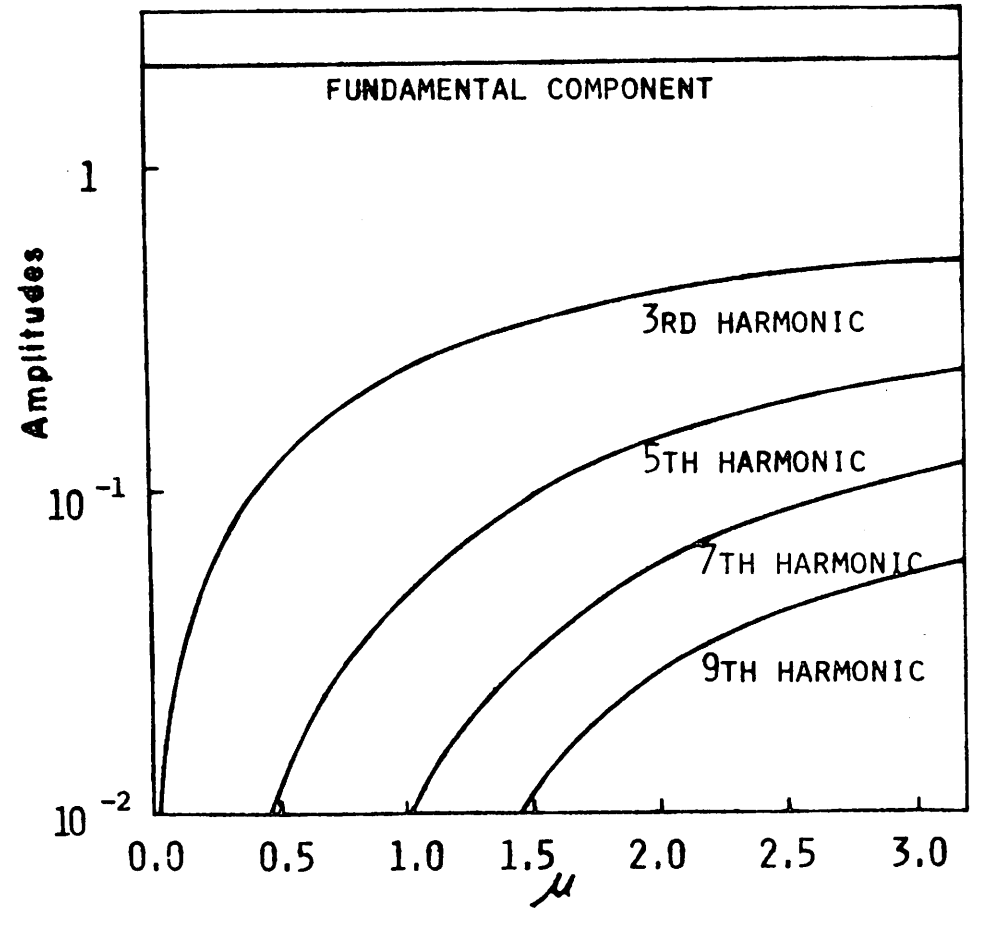
FUNDAMENTAL COMPONENT
1
10^{-1}
10^{-2}
Amplitudes
3RD HARMONIC
5TH HARMONIC
7TH HARMONIC
9TH HARMONIC
0.0
0.5
1.0
1.5
2.0
2.5
3.0
μ

(b)

Fig. 12